

11-14-1980

Electrostatic TEM Studies of Magnetic Domains in Thin Iron Films

Hideaki Karamon
Portland State University

Follow this and additional works at: https://pdxscholar.library.pdx.edu/open_access_etds



Part of the [Atomic, Molecular and Optical Physics Commons](#)

Let us know how access to this document benefits you.

Recommended Citation


Karamon, Hideaki, "Electrostatic TEM Studies of Magnetic Domains in Thin Iron Films" (1980).
Dissertations and Theses. Paper 2963.
<https://doi.org/10.15760/etd.2957>


This Thesis is brought to you for free and open access. It has been accepted for inclusion in Dissertations and Theses by an authorized administrator of PDXScholar. Please contact us if we can make this document more accessible: pdxscholar@pdx.edu.


AN ABSTRACT OF THE THESIS OF Hideaki Karamon for the Master of Science
in Physics presented November 14, 1980.

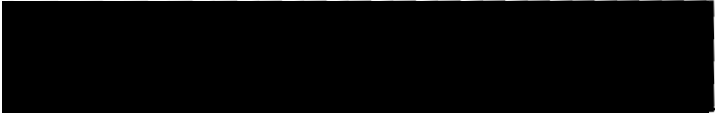
Title: Electrostatic TEM Studies of Magnetic Domains in
Thin Iron Films.

APPROVED BY MEMBERS OF THE THESIS COMMITTEE:


John Dash, Chairman


Gertrude Rempfer


Makoto Takeo


Charles M. McIntyre

An electron microscope with electrostatic lenses was used for
high resolution studies of magnetic domains in thin iron films.

Observation methods used to determine the directions of local
magnetization in iron thin films were the Lorentz method and the
Foucault method.

We studied how Bloch line-crosstie pairs and crosstie main walls

behave in applied, in-plane magnetic fields. We found that crosstie main walls remain unchanged until crosstie density goes nearly to zero when the field is applied perpendicular to the main wall. A twisted type of domain appears where crossties disappear.

We also succeeded in observing an annihilation process of Bloch line-crosstie pairs in the field application.

Crosstie-twisted boundaries were analyzed to determine the directions of local magnetization by both the Lorentz method and the Foucault method. We found in this study that crosstie-twisted boundaries are combinations of 90° domain walls, 180° domain walls and crosstie walls. Crossties do not appear along 90° domain walls, but do appear along 180° walls. The crosstie density along 180° walls is approximately 4500 cm^{-1} .

ELECTROSTATIC TEM STUDIES OF MAGNETIC DOMAINS
IN THIN IRON FILMS

by

Hideaki Karamon

A thesis submitted in partial fulfillment of the
requirements for the degree of

MASTER OF SCIENCE
in
PHYSICS


Portland State University


1980

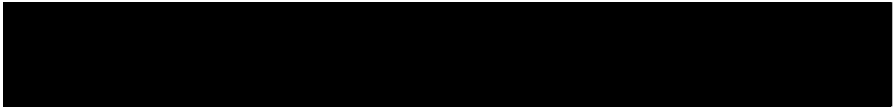
TO THE OFFICE OF GRADUATE STUDIES AND RESEARCH:

The members of the Committee approve the thesis of
Hideaki Karamon presented November 14, 1980.

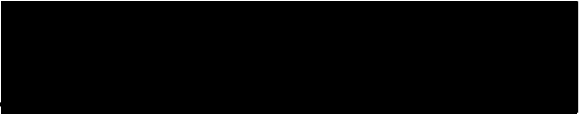

John Dash



Gertrude Rempfer


Makoto Takeo


Charles M. McIntyre

APPROVED:


Mark Gurevitch, Head, Department of Physics


Stanley E. Rauch, Dean of Graduate Studies and Research

ACKNOWLEDGEMENTS

I wish to express great appreciation and many thanks to Professors G. Rempfer and J. Dash for their invaluable guidance and encouragement.

I also wish to thank Professor M. Takeo for valuable discussions.

I would like to thank K. Mensah of Tektronix Inc. for assistance in measuring the film thickness.

Hideaki Karamon

A Beautiful Rainy Day, in Portland. OR.

TABLE OF CONTENTS

	PAGE
ACKNOWLEDGMENTS	iii
LIST OF FIGURES	vi
 CHAPTER	
I INTRODUCTION	1
II EXPERIMENTAL METHODS	6
Specimen Preparation and Experimental Set Up	6
Lorentz Method (Defocus Method)	11
Foucault Method (Schlieren Method)	15
III EXPERIMENTAL RESULTS AND DISCUSSION	20
Observation of Magnetic Domains by Use of a TEM and an ETEM	20
Determination of the Direction of the Local Magnetization of Crosstie Walls by the Lorentz Method	25
Determination of the Direction of the Local Magnetization of Crosstie Walls by the Foucault Method	30
A Study of the Effect on Crosstie Walls of an In-plane Magnetic Field	35
A Study of Bloch line-crosstie Annihilation in an Applied Magnetic Field	40

CHAPTER

A Study of Twisted Type Domains and Crosstie-twisted Boundaries	43
IV SUMMARY AND CONCLUSIONS	52
REFERENCES	53

LIST OF FIGURES

FIGURE	PAGE
1. Diagrams Illustrating the Scratch Technique for Determination of the Direction of Magnetization	3
2. Schematic Diagram of the Evaporator System Which Was Used for Preparation of the Thin Film . .	7
3. HITACHI E.M. TYPE HS-7S	8
4. ELEKTROS ETEM 101	8
5. Side View of the Solenoid Used for Applying a Magnetic Field to the Specimen	10
6. (a) Schematic Diagram Showing the Deflection of the Incident Electron Beam by Domains of Opposite Type. (b) Transmitted Beam Intensity in the Plane of the Overfocus Image and (c) in the Plane of the Underfocus Image	13
7. Examples of Micrographs of an Iron Thin Film Observed by the Lorentz Method with an ETEM .	14
8. The Direction of Magnetization in the Specimen Plane Is into the Paper. δ Indicates a Distance Between the Z-Axis and a Point Through Which Electrons Pass in the Rear Focal Plane . . .	16

9.	Three-dimensional Illustration of the Foucault Method	18
10.	Three-dimensional Illustration of the Foucault Method. This Figure Shows the Effect of Opposite Directions of Magnetization in the Specimen and the Aperture Displaced Slightly to the Right	19
11.	Objective Lens Axial Magnetic Field Around a Pole Piece	21
12.	Domain Patterns Observed in the Same Area (a) First with TEM and (b) Subsequently with ETEM	22
13.	Domain Patterns Observed in the Same Area (a) First with ETEM and (b) Subsequently with TEM	23
14.	Underfocused Micrograph of Crosstie Walls in a Thin Iron Film	26
15.	(a) Shows a Schematic Illustration of Figure 14. (b) Indicates Vector Components of Local Magnetization Which Can Account for the Observed Domain Wall Contrast	27
16.	Relationship Between Directions of Local Magnetization and Electron Micrograph Contrast	28

FIGURE

17.	Sum of Vector Components of Local Magnetization in Figure 15(b)	29
18.	Crosstie Model Postulated by E. E. Huber, et al.	29
19.	(a) Indicates the Directions of the Objective Aperture Displaced Slightly off the Optical Axis and the Directions of Given Local Magnetizations in a Specimen. (b) Shows Bright and Dark Areas in the Focused Images Obtained by the Aperture Displacement Corresponding to the above Illustration in (a)	31
20.	Contrast on the Focused Image Obtained by the Foucault Method	32
21.	(A), (B) and (C) Show Illustrations of the Contrast in Figure 20(a), (b) and (c). (A'), (B') and (C') Indicate the Directions of Local Magnetizations Which Account for the Corresponding Contrast in (A), (B) and (C) .	33
22.	(a) Shows the Combination of Local Magnetization Obtained in Figure 21. (b) Indicates the Vectorial Sum of Local Magnetization in (a) .	34
23.	Relation Between (a) Crosstie Density and Applied Field Normal to the Crosstie Main Wall, and (b) Field Dependence on Crosstie Main Wall-Wall Distance	36

24.	Field Dependence of Crosstie Walls in an Iron Thin Film by the Underfocus Method (a), (b), and (c)	37
24	Field Dependence of Crosstie Walls in an Iron Thin Film by the Underfocus Method (d), (e), and (f)	38
25.	Field Dependence of Crosstie Walls in an Iron Thin Film by the Underfocus Method. Film Thickness Was $\sim 200 \text{ \AA}$	39
26.	Electron Micrographs of a Bloch Line-crosstie Annihilation in the In-plane Field Dependence	41
27.	Illustration of a Bloch Line-crosstie Annihilation in the In-plane Field Dependence in Figure 26	42
28.	Energy per Unit Area of a Bloch Wall, a Néel Wall and a Crosstie Wall As a Function of the Film Thickness (Permalloy Thin Films).	44
29.	Twisted Domains with No Intentional Field Application, Which Occur at $\sim 200 \text{ \AA}$ Thickness in Iron Thin Film	45
30.	Crosstie-twisted Boundaries with No Intentional Applied Field Occur at $\sim 200 \text{ \AA}$ Thickness in Iron Thin Film	45

FIGURE

PAGE

31.	The Same Crosstie-twisted Boundaries with No Intentional Field Application in Figure 30 Were Subsequently Taken by the Foucault Method	46
32.	Illustration of Crosstie-twisted Boundaries Observed by the Underfocus Method in Figure 30	49
33.	Relation Between the Contrast of a Thick or Thin line and Directions of Local Magnetization .	50
34.	Possible Configuration of Magnetization of Crosstie-twisted Boundaries	51

CHAPTER I

INTRODUCTION

In ferromagnetic materials at room temperature there exist regions in which cooperative interactions result in the spontaneous alignment of the magnetic moments of large numbers of atoms. These regions are called domains and are magnetized locally to saturation even in the absence of an external field. In an unmagnetized specimen the directions of magnetization are not the same in all domains and the resultant magnetic moment as a whole is zero.

P. Weiss postulated a magnetic domain structure in 1907. Since that time interesting studies on magnetic domains have been actively pursued both theoretically and experimentally by a number of investigators. These studies provided evidence for a domain structure in which the magnetization direction was parallel to the boundary between domains and alternated from one domain to the next.

The first observation of magnetic domains was made by F. Bitter (1) in 1931. He reported studies on iron, nickel, and an iron-silicon alloy. He used a colloidal suspension consisting of Fe_3O_4 fine magnetic particles (Fe_2O_3 is indicated in his paper) to explore the magnetic properties of a specimen. The colloidal suspension was placed on the specimen and observation was made with an optical microscope. The colloidal particles collected in regions of magnetic field inhomogeneity, for example near topographical features on the specimen surface and along

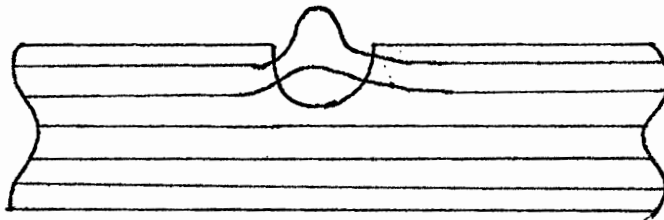
domain boundaries. This made possible the visualization of magnetic fields at the specimen surface.

In his famous papers "On Inhomogeneities in the Magnetization of Ferromagnetic Materials (1)" and "Experiments on the Nature of Ferromagnetism (2)," Bitter described the appearance of inhomogeneities and irregularities in the specimens, but did not mention that these were probably the first observations of magnetic domains. This method of observing magnetic domains is usually called the Bitter colloidal technique.

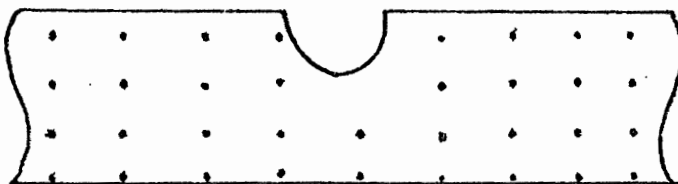
One of the applications of the Bitter technique introduced by H. J. Williams, R. M. Bozorth and W. Shockley (3) was to determine the direction of local magnetization. This was done by making a microscopic scratch across the specimen surface with a very fine glass fiber and observing the pattern in which the colloidal particles collected. Diagrams of a scratched crystal surface are shown in Figure 1(a) and (b). Figure 1(a) shows a scratch perpendicular to the magnetization and magnetic flux emerging from the surface. In Figure 1(b) the direction of magnetization is parallel to the scratch and there is no flux emerging. In case (a) the inhomogeneous stray magnetic field due to the scratch attracts magnetic colloidal particles along the scratch, whereas in case (b) particles do not collect along the scratch. This is but one illustration of the use of the Bitter colloidal technique.

Following Bitter's observation of magnetic domains by this method, the colloidal technique has been widely applied in the study of magnetic fields at surfaces of magnetic specimens, and has contributed greatly to the study of magnetic domains.

Magnetic domains were first observed using bulk specimens. Later



(a)



(b)

Figure 1(a),(b). Diagrams illustrating the scratch technique for determination of the direction of magnetization.

In (a) the magnetization is perpendicular to the scratch, and the emerging magnetic flux attracts the colloidal particles.

In (b) the magnetization is parallel to the scratch and there is no flux emerging.

on, the Bitter technique was applied also to the study of magnetic domains in thin films, where the patterns in which the colloidal particles collect delineate the boundaries, or walls, between domains.

Thin magnetic films up to $\sim 1000 \text{ \AA}$ thick (or above depending on accelerating voltage) can also be studied by direct observation in the transmission electron microscope (TEM). In this method the Lorentz force on an electron passing through the magnetic field of the specimen provides a means for determining the field direction and for distinguishing regions of different magnetizations. The first observation was made by M.E.Hale, H.W.Fuller, and H.Rubinstein (4). They demonstrated that the electron optical method had a very promising future for the study of magnetic domains. Hale et al. used a Phillips EM-75 B magnetic type electron microscope to study iron and permalloy thin films of $\sim 500 \text{ \AA}$ thickness. H. W. Fuller and M. E. Hale also introduced the use of electrostatic-focusing microscopes (EEM) (5) for the observation of magnetic domains. A great advantage of the electrostatic type of microscope in the study of magnetic thin films is the freedom from magnetic field in the specimen area. By contrast, in the magnetic type microscope, in order to avoid interference by magnetic fields, the specimen must be located outside the strong magnetic field of the objective lens, and the focal power of the lens must be correspondingly reduced. The first observations by EEM were made with the AEG-Zeiss and Trüb-Täuber instruments.

After the pioneering experiments of Hale et al., a number of interesting studies of magnetic domains in thin films by means of TEM have been published (6, 7, 8, 9, 10, 11, 12, 13).

In thin films (200 \AA - 2000 \AA thick depending on material and

treatment) the domain walls can have complex structure such as crossties where components of the magnetization in the plane of the film cross the main walls and produce regions where the magnetic field circulation is not zero. The axis of such a region, normal to the surface of the film, is called a Bloch line. The subject of this thesis is largely concerned with observation of crosstie walls and Bloch lines by ETEM.

Crossties were first observed by E. E. Huber, Jr., D. O. Smith and J. B. Goodenough (14) using the Bitter technique. Following this, numerous further studies of crosstie walls by the Bitter technique (e.g. 15, 16, 17, 18, 19, 20, 21, 31) have been published. Crossties have also been studied by the TEM technique (5, 22, 23, 24, 25, 26).

Technologically speaking, a series of studies on the use of a permalloy strip as a data track for a crosstie memory was developed by L. J. Schwee et al. (19, 20, 27), R. N. Lee et al. (28) and D. S. Lo et al. (29). This has been one of the interesting technological studies in this period of time. Use of electron microscopes and observation methods will play an important role in the study of crosstie memory devices.

Our studies include : 1. a comparison of the effectiveness of electrostatic and magnetic electron microscopes in studying magnetic domains; 2. the observation of domain boundaries and direction of magnetization; 3. the effect of an in-plane magnetic field on the crosstie-Bloch line structure and on the domain wall movement; 4. the observation and analysis of twisted domains.

Some of the results were reported at the Electron Microscopy Society of America annual meeting in 1979 (30).

CHAPTER II

EXPERIMENTAL METHODS

1. Specimen Preparation and Experimental Set Up

The material studied in this investigation was pure iron (99.998 % Fe). The specimens were prepared by evaporating the metal onto microscope glass slides in a vacuum. A pressure of approximately $2-3 \times 10^{-5}$ mmHg was maintained during evaporation. The vacuum evaporator is shown in Figure 2. The glass slides used in these experiments were washed with distilled water, rinsed with acetone, and dried in air in order to make their surfaces clean and smooth. A mass of 20 mg Fe foil (125 μ m thick) was placed in a helical filament of tungsten approximately 7 cm away from the glass slides. At this distance films of $\sim 200 \text{ \AA}$ thickness were produced, in which crosstie walls could be observed. The thin films were floated off the glass slides onto the surface of distilled water, and picked up on 3 mm diameter Cu grids for TEM observation. A HITACHI TEM TYPE HS-7S (50 kv) and an ELEKTROS ETEM 101 (40 kv), shown in Figure 3 and Figure 4 respectively, were used for observation of the specimens.

For a study of the effect of external magnetic fields on the domains, a solenoid was constructed as shown in Figure 5. The specimen was placed in the center of the solenoid, oriented so that the solenoid axis was parallel to the specimen surface. A calculation of the magnetic field in the solenoid was made by application of the Biot-Savart law,

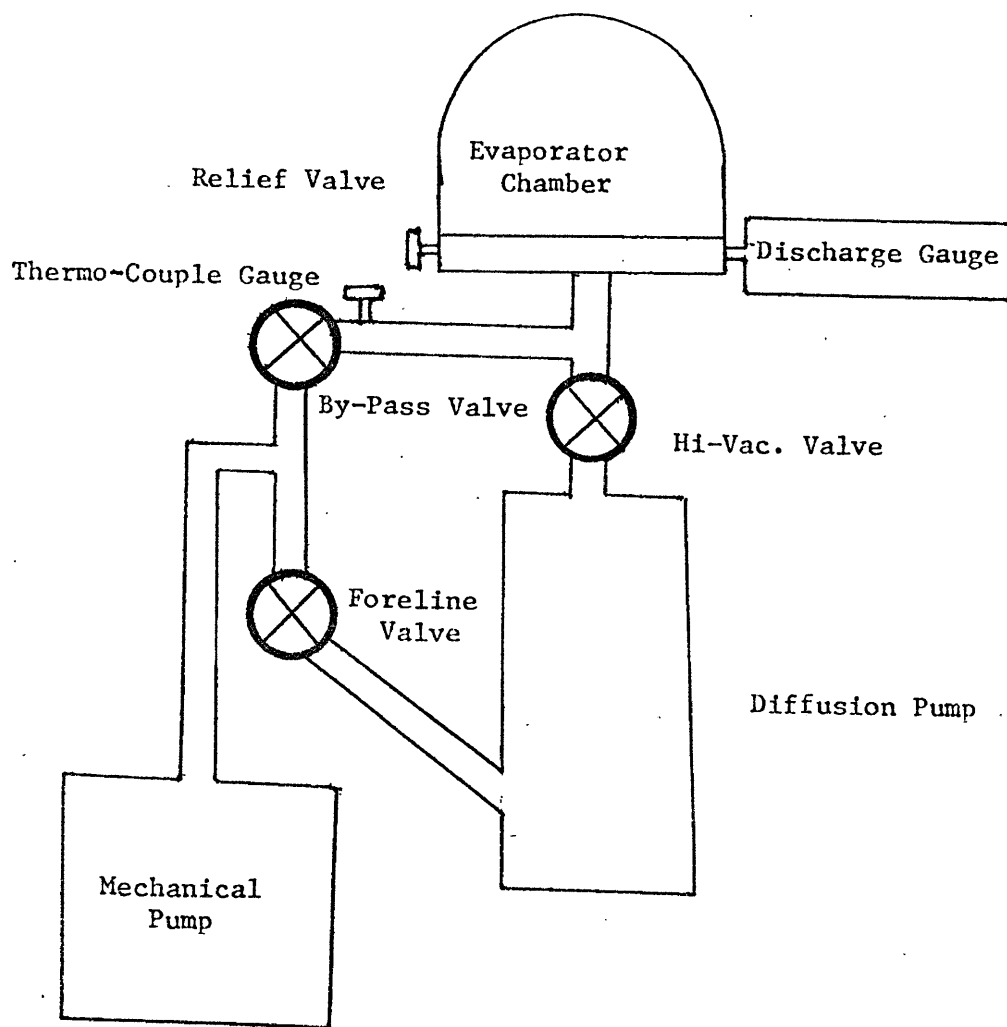


Figure 2. Schematic diagram of the evaporator system which was used for preparation of the thin films.

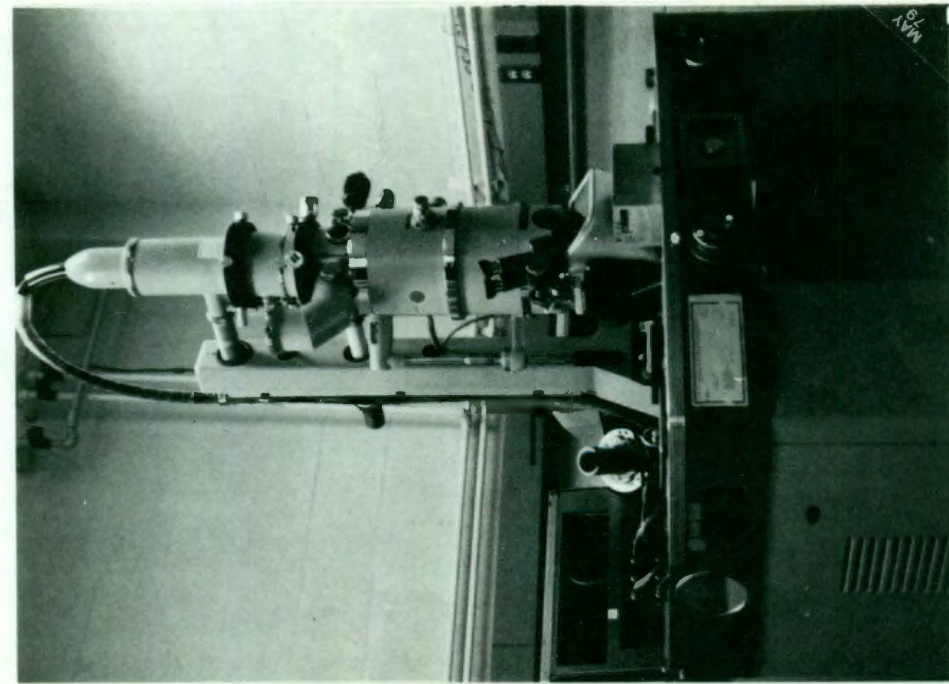


Figure 3. HITACHI E.M. TYPE HS-7S

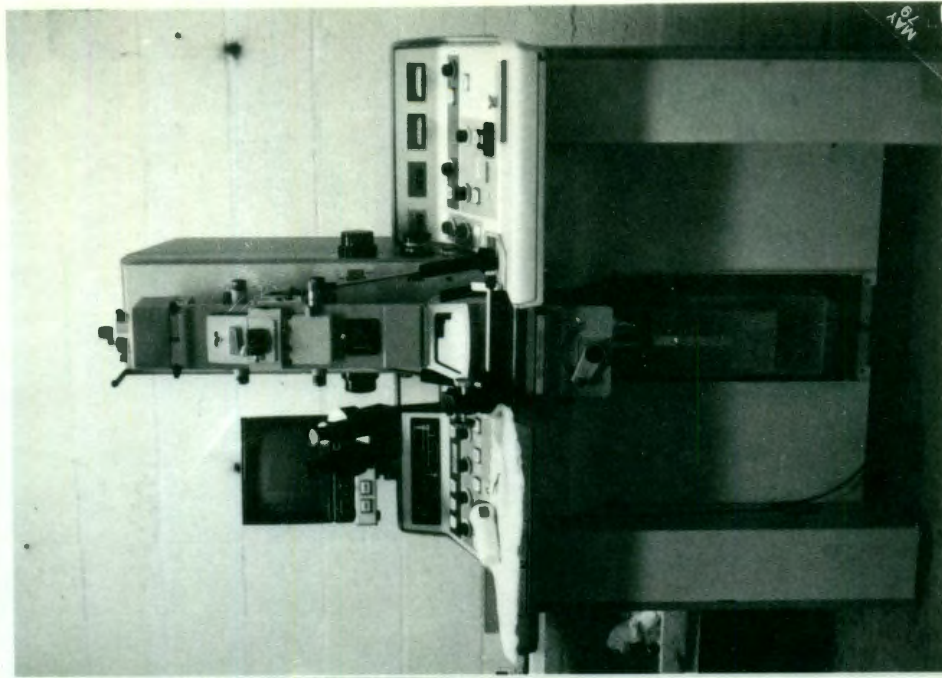


Figure 4. ELEKTROS ETEM 101

in MKS system of units,

$$H = \frac{N I}{2 L} (\cos \phi_2 - \cos \phi_1) \quad \text{on the axis.}$$

$$H_o = \frac{N I}{L} \cos \phi_2 \quad \text{at the center the solenoid.}$$

Inserting the numerical values, $N = 500$ turns, $L = 1.08 \times 10^{-1}$ m, and $\phi_2 = 10.5^\circ$, we find

$$H_o = 4.5 \times 10^3 I \quad \text{AT/m}$$

$$= 57I \text{ Oe}, \text{ and } I \text{ is in amperes}$$

$$\text{where } 1 \text{ AT/m} = 4\pi \times 10^{-3} \text{ Oe.}$$

For thickness measurement of specimens a Reichert Nomarski Type Interferometer was used.

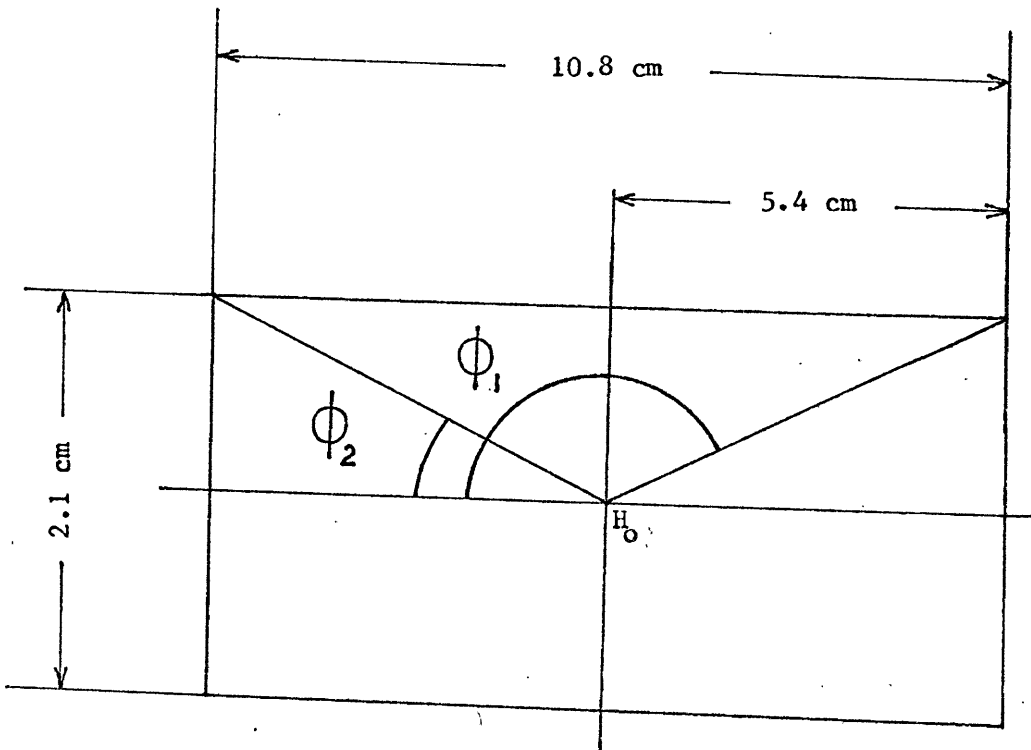


Figure 5. Side view of the solenoid used for applying a magnetic field to the specimen. H_0 is the field at the center of the solenoid. The radial dimension has been exaggerated for clarity.

Following are the methods which were used to obtain magnetic domain contrasts:

2. Lorentz Method (Defocus Method) (4)

Electrons passing through a magnetic film experience a force

$$\vec{F} = \frac{4\pi e}{c} (\vec{v} \times \vec{M}) \quad \text{in the Gaussian system of units}$$

where v is the electron velocity, M the local magnetization of the specimen, e the electron charge, and c the speed of light. This force in general causes a deflection of the electron beam. The amount of beam deflection depends on the film thickness, the local magnetization in the film and the accelerating voltage. Taking the normal to the specimen plane to be in the z -direction and assuming normal incidence for the electron beam, the deflection angle (5) can be expressed in the form

$$\phi_x = \left[\frac{4\pi M_y}{c} \right] \left[\frac{e}{2 m_0 V} \right]^{1/2} \cdot \left[1 + \frac{eV}{2 m_0 c^2} \right]^{-1/2}$$

where m_0 is the electron rest mass, V the accelerating voltage, and τ the film thickness. In this expression the component of magnetization in the plane of the film is assumed to be in the direction of the y -axis. For an accelerating voltage of 50 kv the last factor in the expression for ϕ_x differs from 1 by only about 2 %, and the deflection can be approximated by

$$\phi_x = \left[\frac{4\pi M_y}{c} \right] \left[\frac{e}{2 m_0 V} \right]^{1/2} \quad (1)$$

In a typical thin film specimen of iron, $M = 1700$ Oe, and if we take $\tau = 250 \text{ \AA}$ and $V = 40$ kv the angular deflection ϕ_x obtained from Eq. (1)

is 8×10^{-5} rad. The deflection produced by the magnetization of the specimen is illustrated in Figure 6(a) for a thin film in which there are domains with alternating directions of magnetization. The direction of magnetization is into the paper in regions (I) and (III) and out of the paper in region (II). The incident electron beam is perpendicular to the plane of the film. Electrons are deflected to the left in regions (I) and (III) and to the right in region (II) as shown. These deflections cause a separation of the parts of the beam which pass through regions (I) and (II) and an overlapping of the parts of the beam which pass through regions (II) and (III). When such a specimen is studied in the electron microscope the presence of domain boundaries can be observed in the defocused image. If the microscope is focused on a plane P following the specimen, the electron intensity distribution in the image appears as in Figure 6(b). When the microscope is focused on a plane P' on the other side of the specimen the virtual intensity distribution in this plane is imaged as shown in Figure 6(c), and the contrast in the neighborhood of domain boundaries is reversed. This reversal distinguishes domain boundary contrast from other types of contrast. Since the power of the objective lens must be increased in order to focus on plane P, this condition is termed "overfocused." In like manner the condition of focusing on plane P' is called "underfocused." Examples of overfocused and underfocused images are shown in Figure 7(a) and (b).

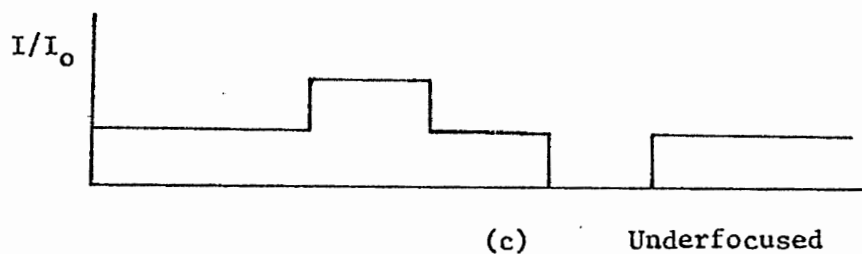
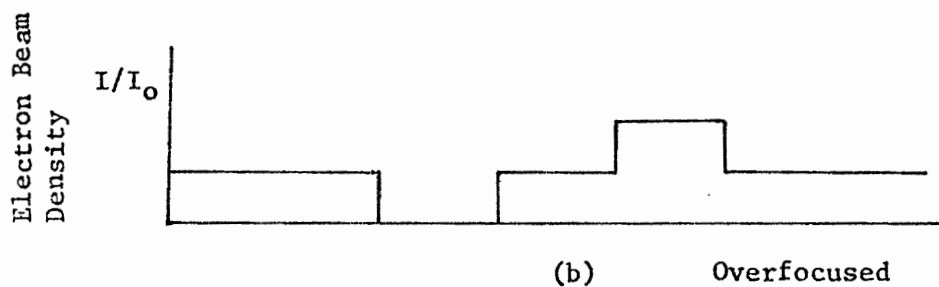
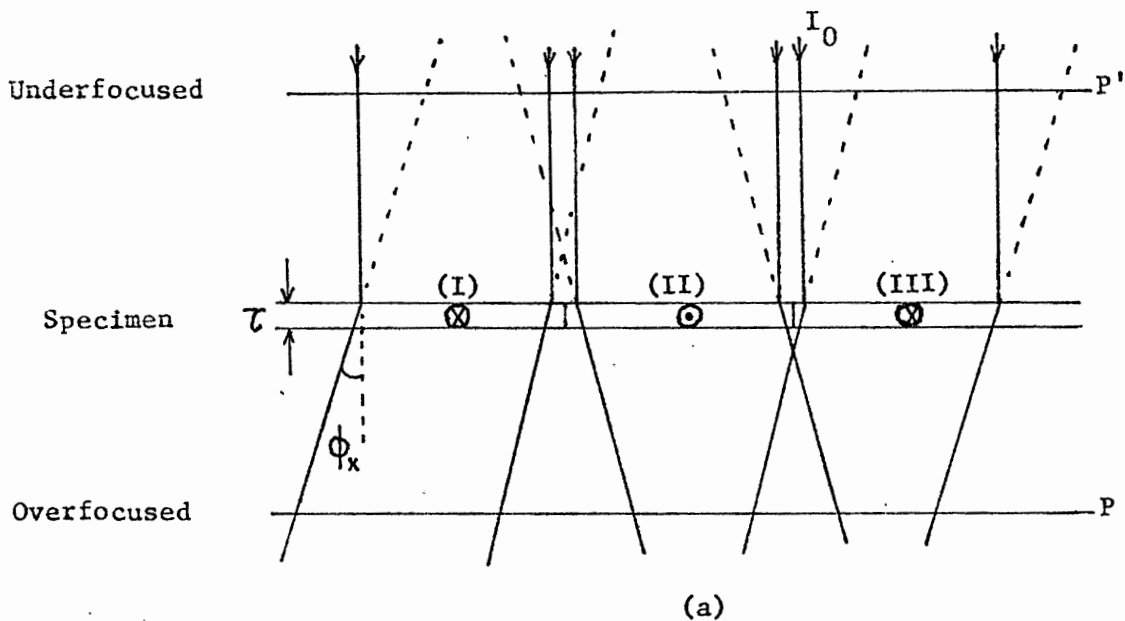
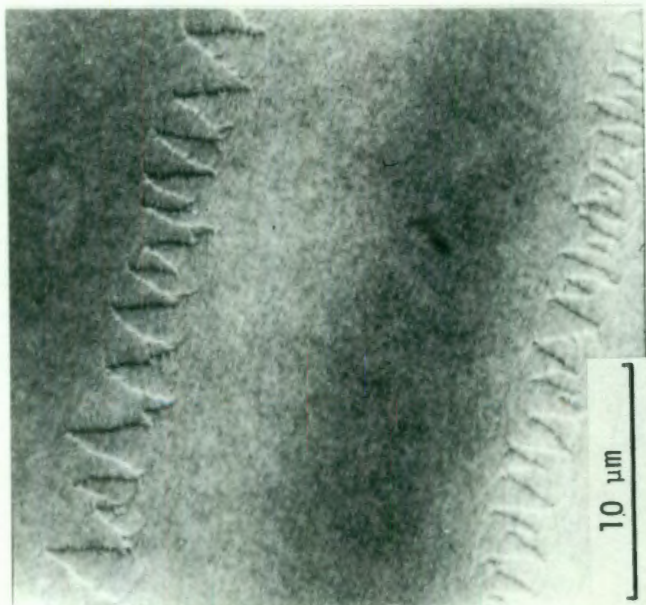


Figure 6. (a) Schematic diagram showing the deflection of the incident electron beam by domains of opposite type (\otimes and \odot). (b) Transmitted beam intensity in the plane of the overfocus image and (c) in the plane of the underfocus image. Deflections are exaggerated for clarity.



(a)



(b)

Figure 7. Examples of micrographs of an iron thin film observed by the Lorentz method with an ETEM. (a) Overfocused image. (b) Underfocused image.

3. Foucault Method (Schlieren Method) (5)

In this method an in-focus image is observed in which the intensity depends on the orientation of the magnetization in the specimen. This type of contrast is obtained through the use of an aperture stop in the rear focal plane of the objective lens. Since electron rays which are deflected in different directions by the specimen pass through different points of the rear focal plane, it is possible by manipulating the aperture diaphragm, or tilting the beam as a whole to selectively intercept certain beams while allowing electrons deflected in other directions to pass through to the image. Thus domains with differing directions of magnetization can, in general, be distinguished by the differing intensities of illumination in the image.

The relation between the angle of deflection and the position in the rear focal plane through which the deflected electrons pass is illustrated in Figure 8. From this diagram we see that electrons deflected through an angle ϕ_x pass through a point in the rear focal plane at a distance δ from the axis, where $\delta = f \cdot \tan \phi_x \approx f \phi_x$. In an electrostatic microscope this point is in the azimuthal plane defined by the direction of deflection and the optical axis. In magnetic microscopes the azimuth of this point is shifted because of the rotation of the electron beam which occurs in the magnetic objective lens.

Three-dimensional illustrations are shown in Figure 9. In (a) the aperture stop is placed at the normal position in the focal plane, so that all of the deflected electrons pass through and produce a bright image. Figure 9(b) shows the effect of displacing the aperture

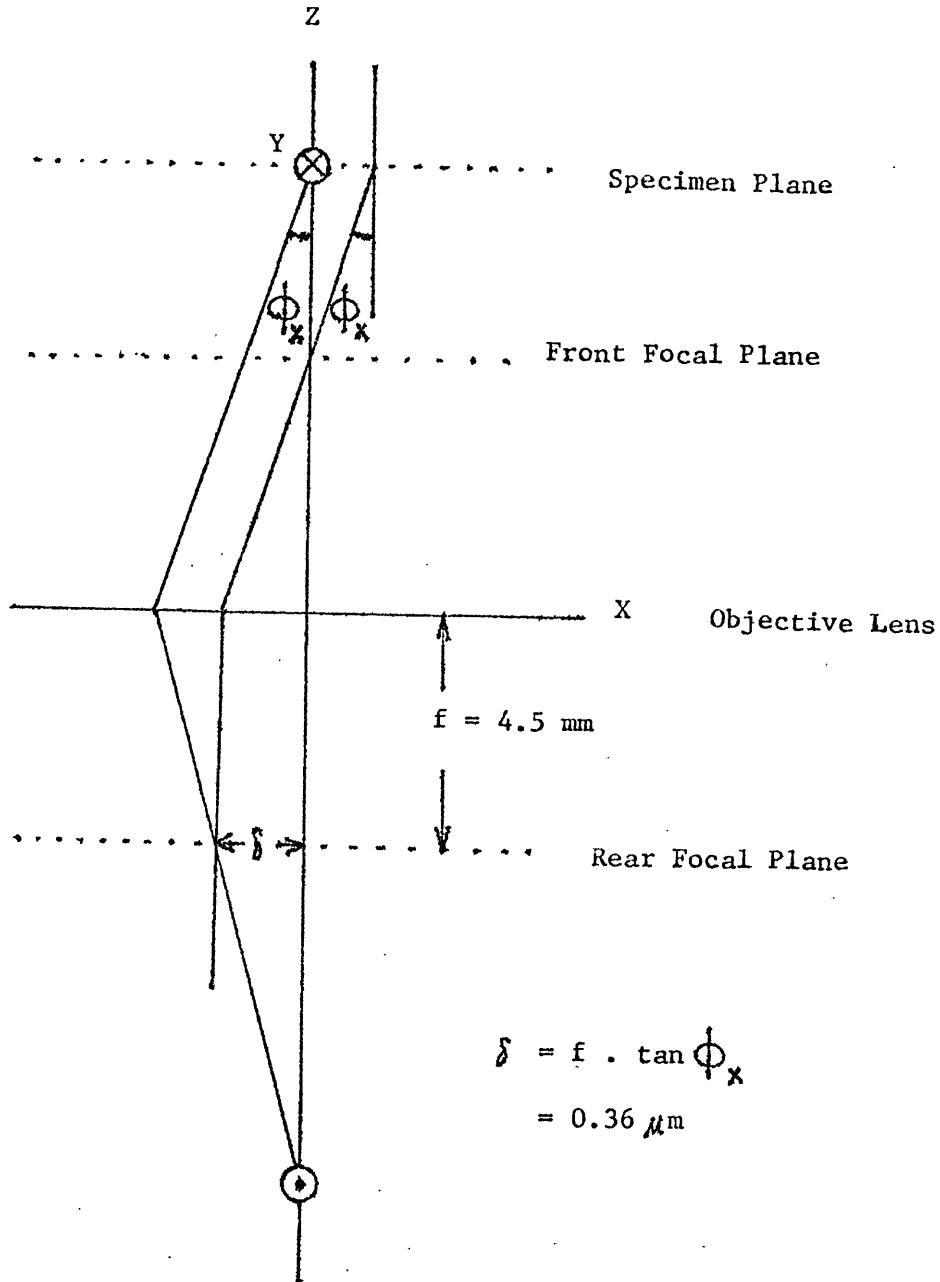


Figure 8. The direction of magnetization in the specimen plane is into the paper. δ indicates the distance between the z-axis and a point through which electrons pass in the rear focal plane.

stop slightly to the right. In this case electrons deflected to the left are blocked by the aperture diaphragm and the image is dark. Figure 10 shows a specimen having two domains with opposite directions of magnetization. Electrons passing through the domain on the left hand side of the specimen are deflected to the left due to the direction of the magnetization as shown. In a similar manner, electrons passing through the domain on the right hand side of the specimen are deflected to the right. Both interception and non-interception of electrons occur in the focal plane with the aperture stop displaced slightly to the right or left, so that bright and dark images can be identified as shown in Figure 10.

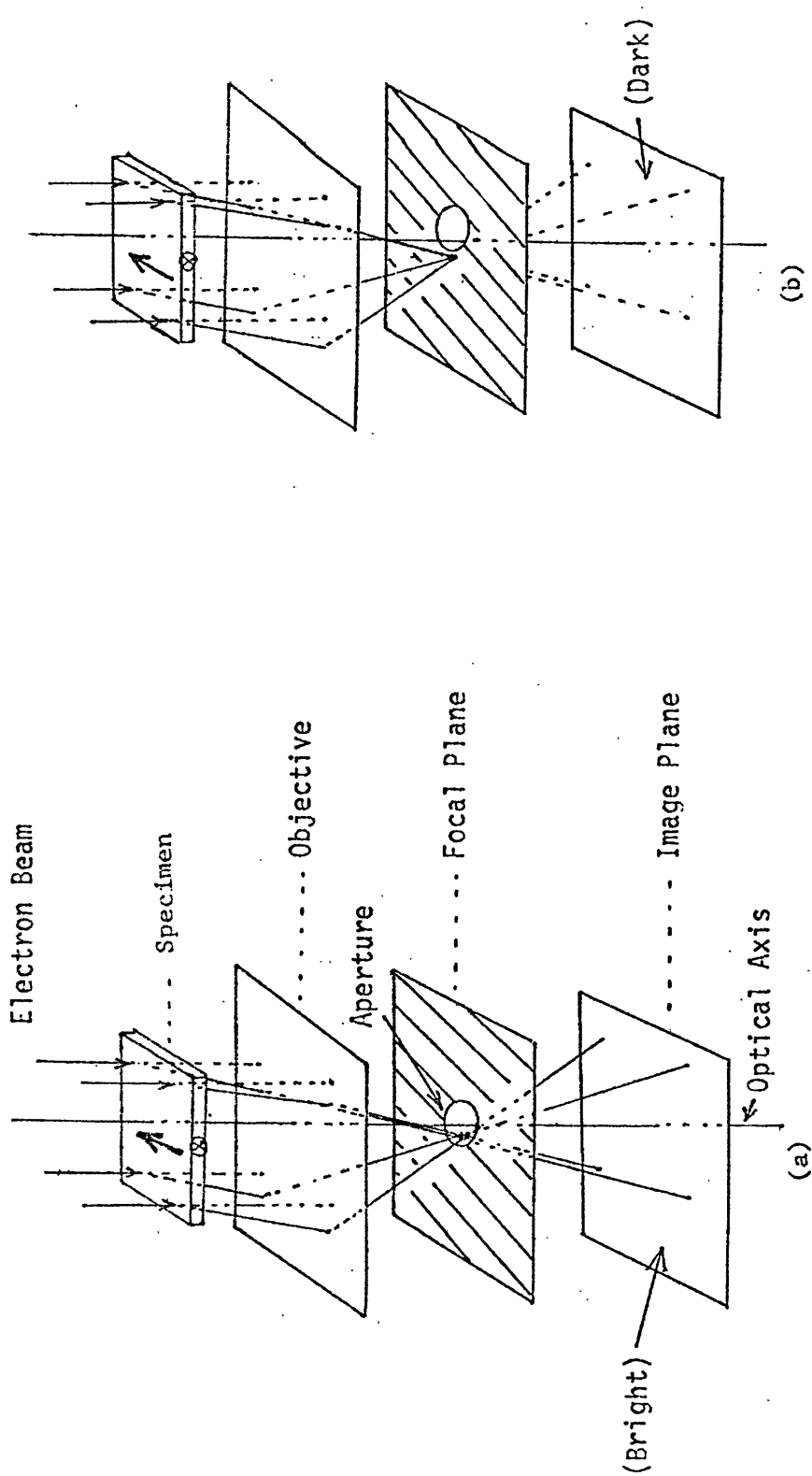


Figure 9. Three-dimensional illustration of the Foucault method.
 (a) shows that the aperture stop is at the normal position.
 (b) indicates the aperture stop displaced slightly to the right.

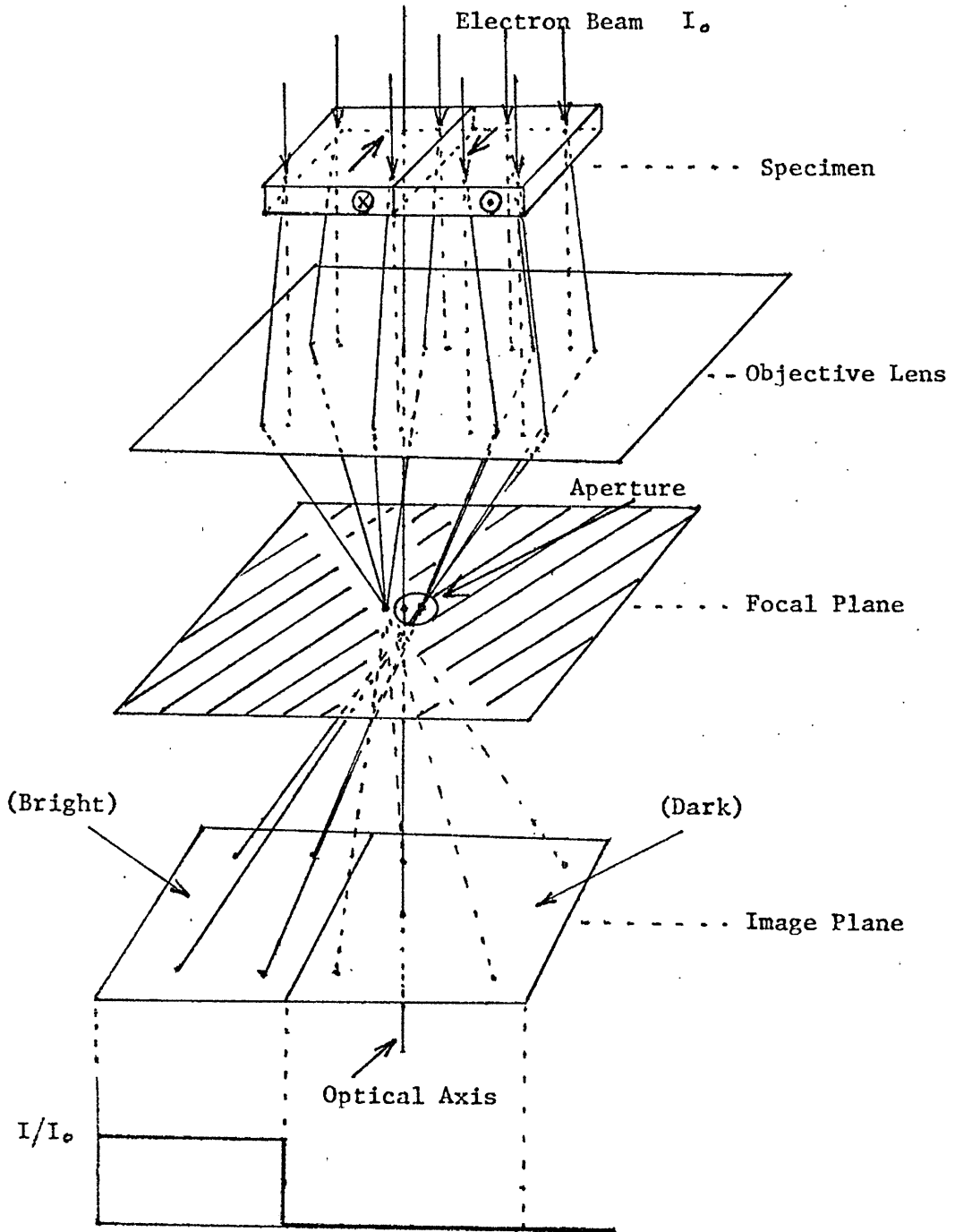


Figure 10. Three-dimensional illustration of the Foucault method. This figure shows the effect of opposite directions of magnetization in the specimen and the aperture displaced slightly to the right.

CHAPTER III

EXPERIMENTAL RESULTS AND DISCUSSION

1. Observation of Magnetic Domains by Use of a TEM and an ETEM

A purpose of this experiment was to compare observations of magnetic domains in a TEM, where the specimen is exposed to a magnetic field, and in an ETEM, where the specimen is in field-free space. A HITACHI TEM (TYPE HS-7S, 50kv) was used as a TEM at full strength of the objective lens. The ETEM used was an ELEKTROS ETEM (TYPE 101, 40 kv). The specimens were studied by the defocus method. Figure 11 illustrates the typical axial magnetic flux measured in the objective lens of a standard HITACHI TEM. The specimen is placed near the top of the objective lens where the axial magnetic flux is in the range of $10 - 10^3$ gauss, depending on how close to the pole piece the specimen is placed.

Micrographs of the same area of a thin iron film were first taken with the TEM and subsequently with the ETEM, as shown in Figure 12(a) and (b). In this process we observed that the two photographs showed the same domains. In the next experiment, the first photograph was taken with the ETEM and subsequently the same area was photographed with the TEM as shown in Figure 13(a) and (b). Drastic changes in the magnetic domains between these photographs can be observed. Domain patterns were often destroyed completely by the magnetic field around

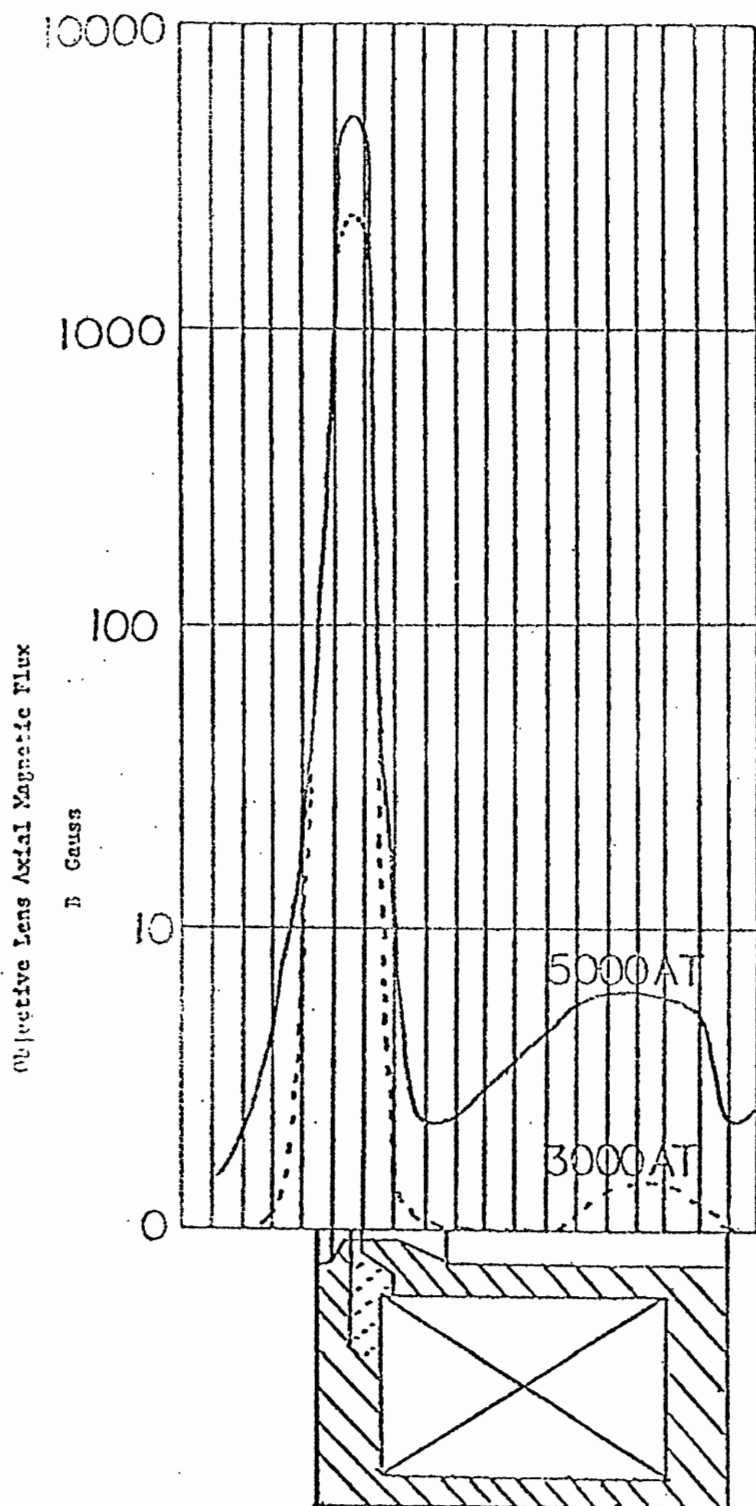
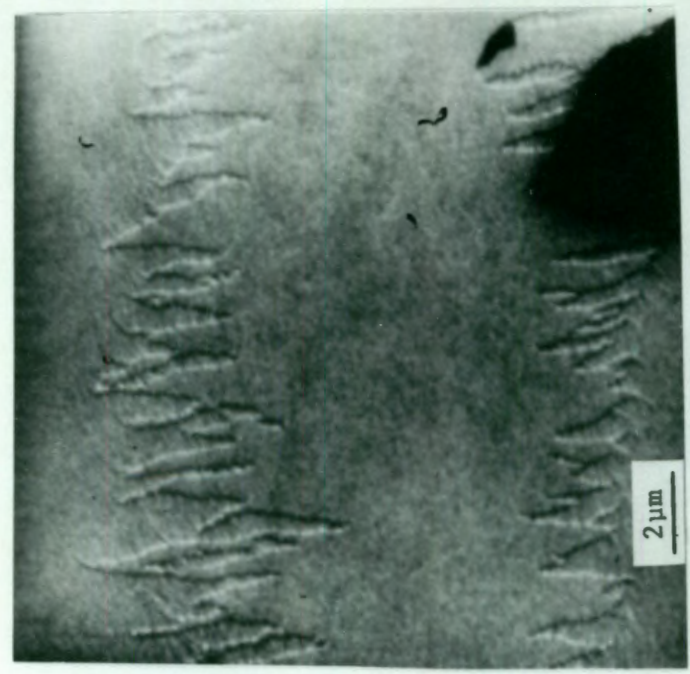


Figure 11. Objective Lens Axial Magnetic Field
Around a Pole Piece (Courtesy of HITACHI)

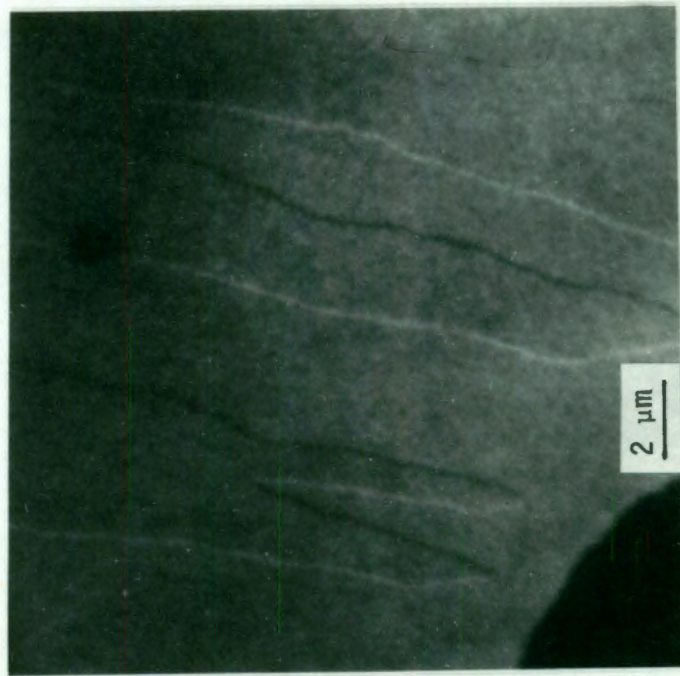


(b)

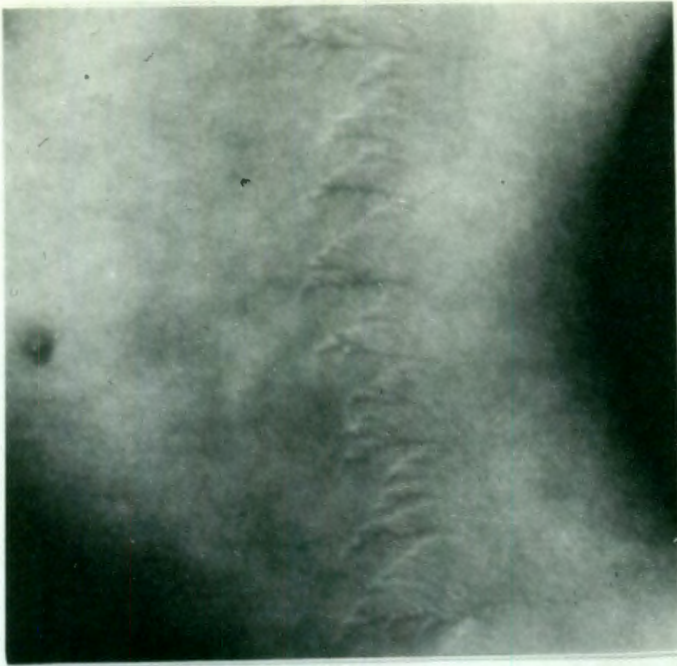


(a)

Figure 12. Domain patterns observed in the same area (a) first with TEM and (b) subsequently with ETEM. This shows that the ETEM does not change domain patterns.



(a)



(b)

Figure 13. Domain patterns observed in the same area (a) first with ETEM and (b) subsequently with TEM. The TEM apparently caused the domain changes.

the specimen area.

As noted in the Introduction, elevating the specimen above the magnetic field of the objective lens makes it impossible to use the TEM at its highest resolution capabilities for magnetic domain studies. This fact has convinced us that ETEM studies show promise of improved resolution in a domain observation technique.

In the ETEM the specimen is in field free space. Thus, the objective lens may be used at full strength without altering ferromagnetic domains. It therefore seems possible that the ETEM will give significantly improved resolution, particularly of the fine structure of magnetic domain walls.

2. Determination of the Direction of the Local Magnetization of Crosstie Walls by the Lorentz Method

In this study observations were made with the ETEM and the underfocus technique was used. An underfocused photograph of crosstie walls in a thin iron film ($\sim 200 \text{ \AA}$ of thickness) is shown in Figure 14. This is schematically illustrated in Figure 15(a). The in-plane magnetization configuration shown in Figure 15(b) was determined by applying the relations between the direction of local magnetization and the underfocused image contrast (Figures 15 and 16). By vector addition of the component vectors parallel and perpendicular to the crossties the configuration turns out to be as shown in Figure 17.

E. E. Huber, et al., (14) who made the first successful observation of crosstie walls by the Bitter technique, postulated a crosstie wall model as shown in Figure 18. Our results, illustrated in Figure 17 for the underfocus method, is consistent with their model in Figure 18.

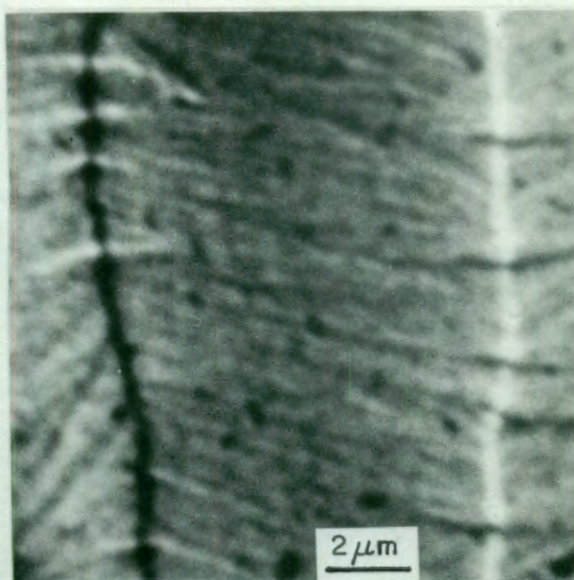
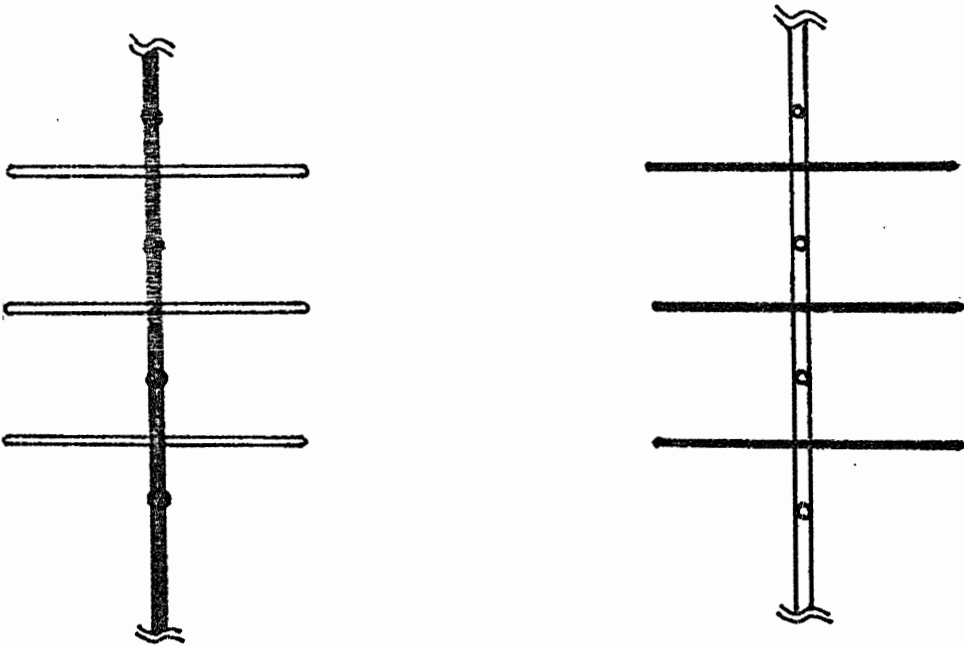
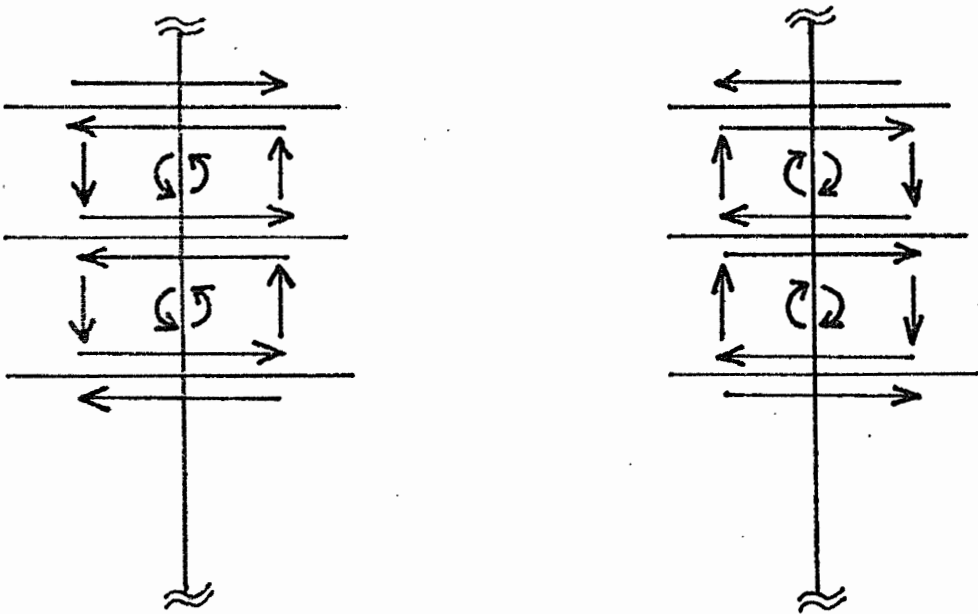


Figure 14. Underfocused micrograph of crosstie walls in a thin iron film ($\sim 200 \text{ \AA}$ of thickness) (30).



(a)



(b)

Figure 15. (a) Shows a schematic illustration of Figure 14. (b) Indicates vector components of local magnetization which can account for the observed domain wall contrast.

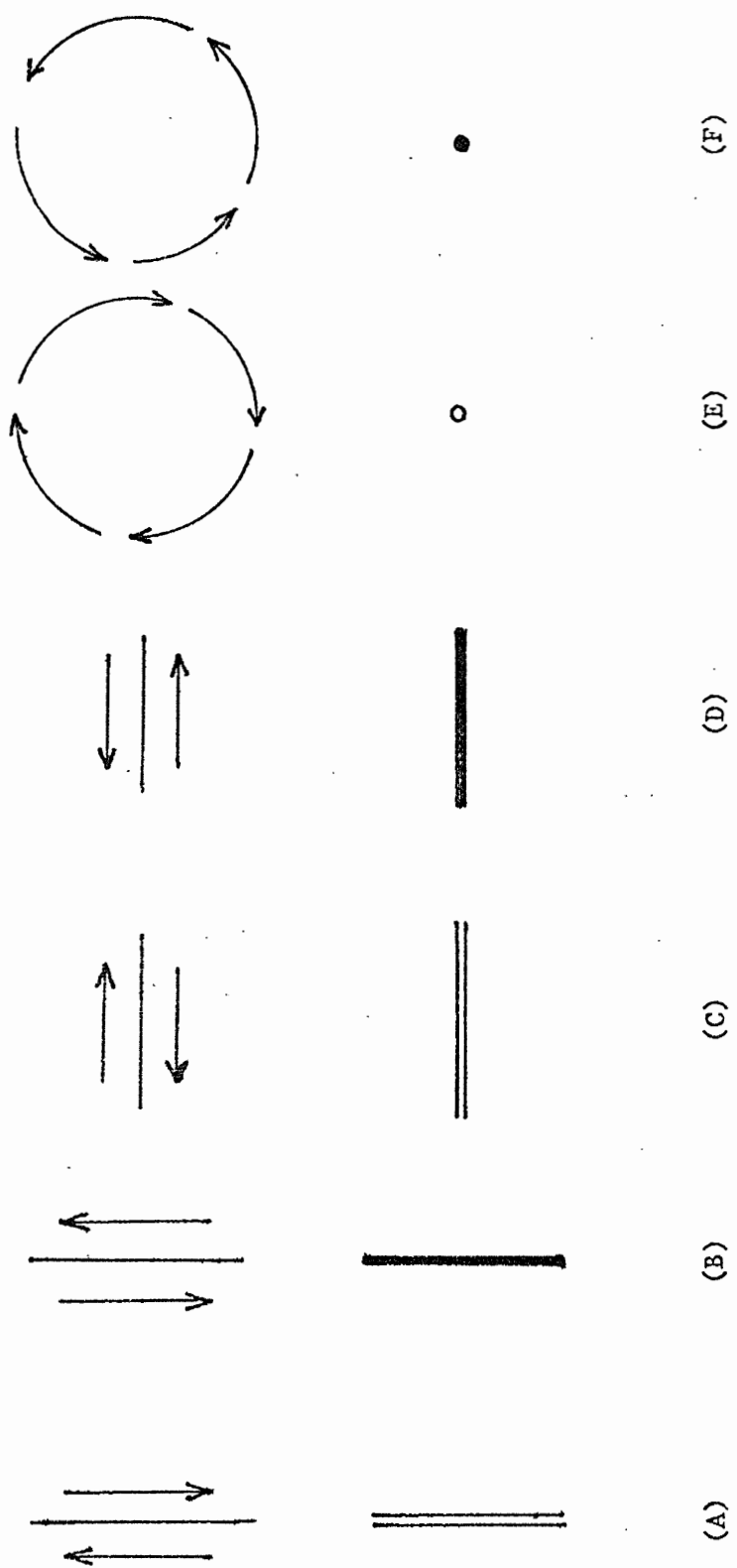


Figure 16. (A), (B), (C) and (D) show relationships between directions of local magnetization parallel to the wall and electron micrograph contrast. (E) and (F) indicate relationships between circular components of local magnetization in the plane and electron micrograph contrast. The contrast shown refers to the underfocused image.

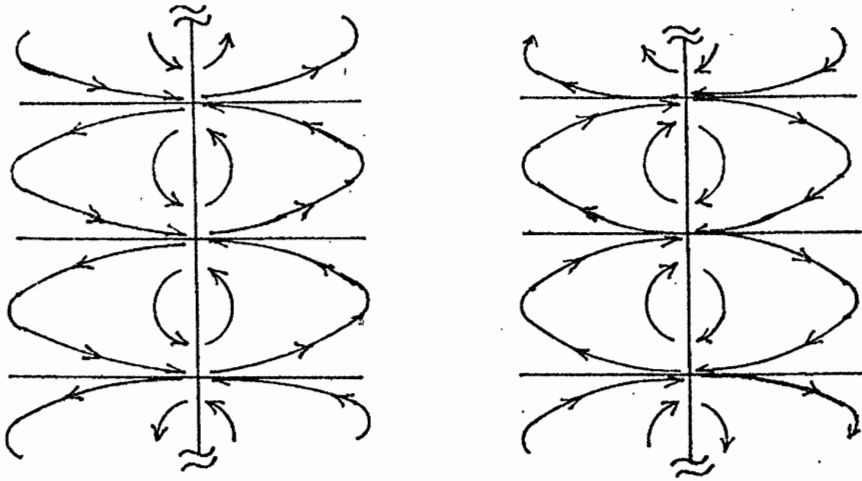


Figure 17. Sum of vector components of local magnetization in Figure 15 (b). This magnetization configuration has some features in common with the crosstie model postulated by E. E. Huber, et al., (14).

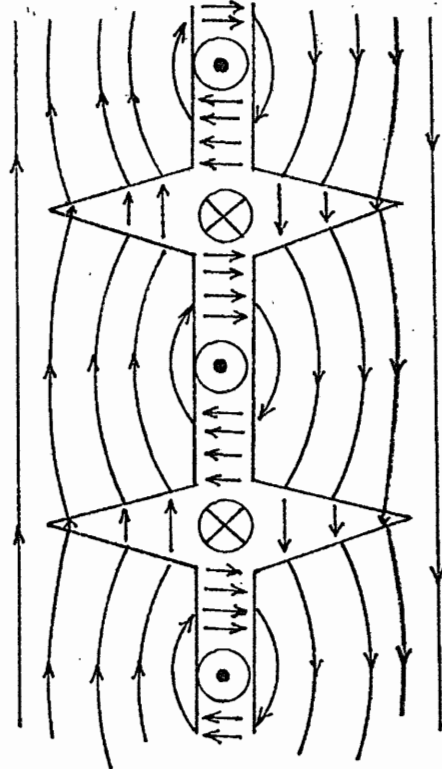


Figure 18. Crosstie model postulated by E.E.Huber, et al., (14).

3. Determination of the Direction of the Local Magnetization of Crosstie Walls by Foucault Method

This method involves an aperture displacement technique with the specimen in-focus, as discussed in Section 3, Chapter II. As illustrated in Figure 19(a) and (b) sharply defined, bright and dark contrasts emerge in the image plane when the objective aperture is displaced slightly off the optical axis. This technique was applied in obtaining the micrographs shown in Figure 20(a), (b), and (c) (30). These micrographs were used to analyze the direction of local magnetization. The directions of local magnetization determined for Figure 20(a), (b) and (c) are illustrated in Figure 21. All the components of local magnetization obtained in Figure 21 were combined in Figure 22(a). Summation of each combination of magnetization components parallel and perpendicular to the crossties gives the resultant configuration which is illustrated in Figure 22(b). This is consistent with the results obtained by the underfocus method illustrated in Figure 18 for the same specimen area. It should be noted that the contrast on opposite sides of the crossties is opposite, as predicted by the Huber model (14). Thus, the Foucault method is one of the most useful techniques for determining the local magnetization. Because it is a high resolution technique, it gives information which nicely complements that obtained by the out-of-focus method.

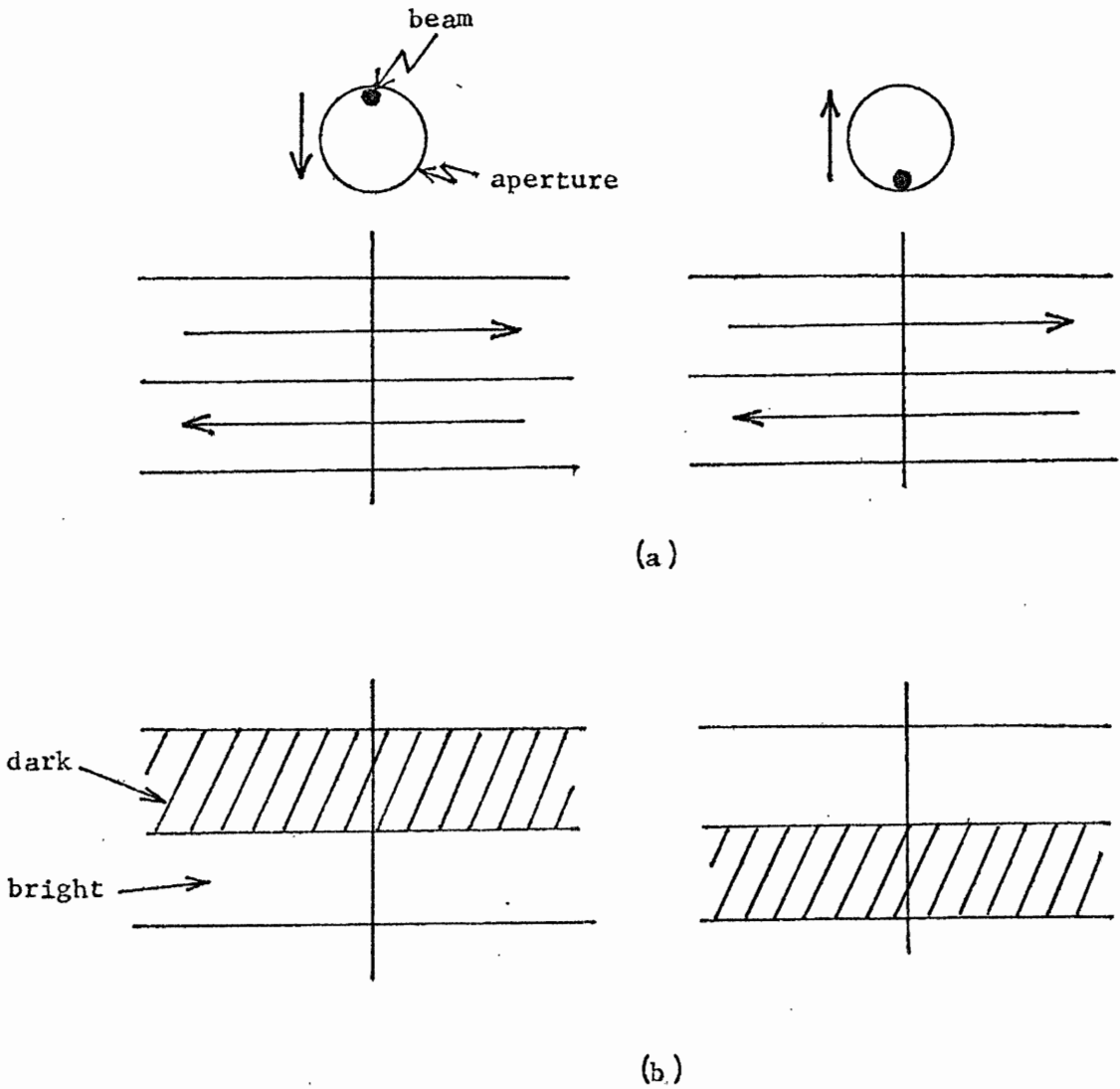
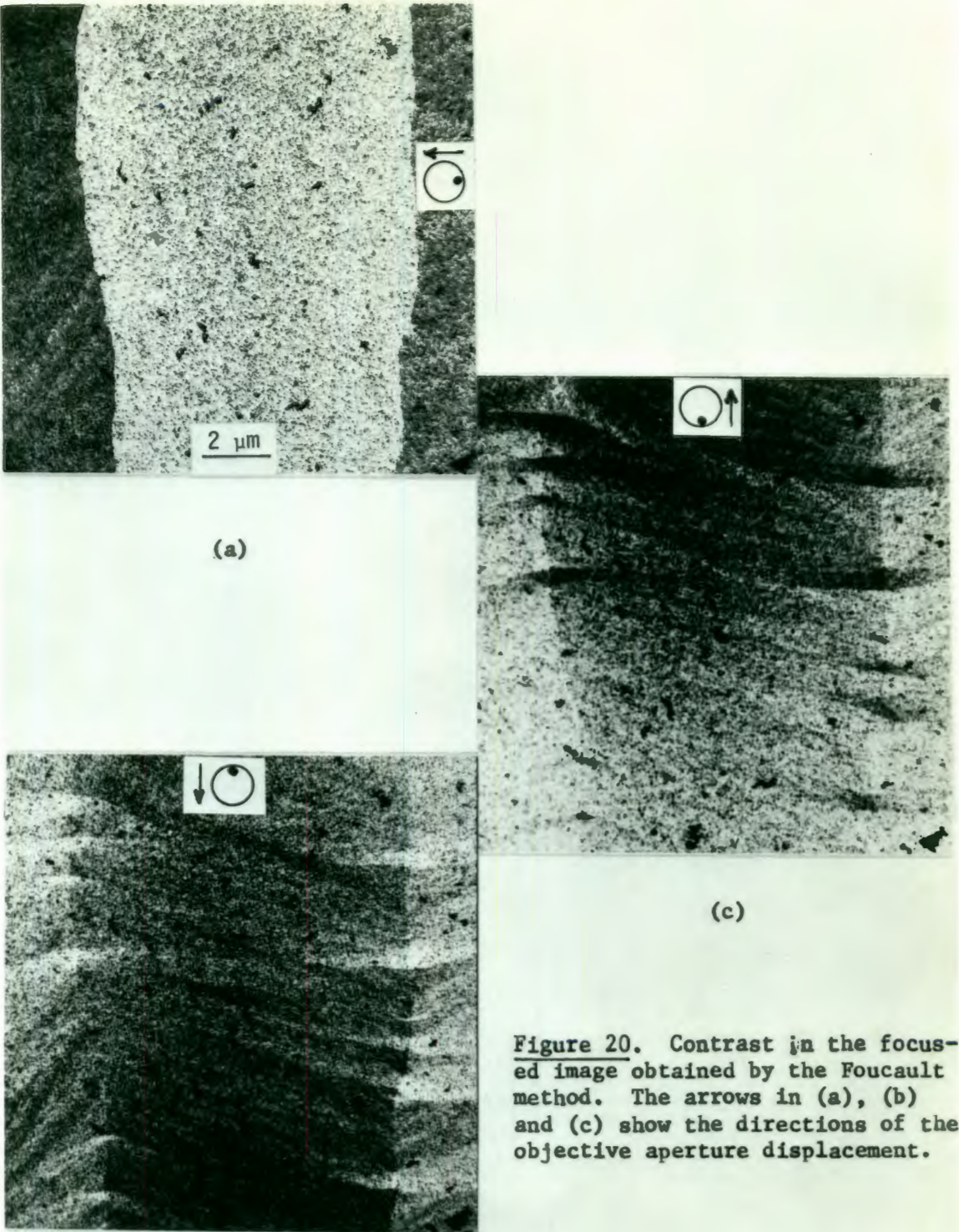


Figure 19. (a) Indicates the directions of the objective aperture displaced slightly off the optical axis and the directions of given local magnetizations in a specimen. (b) Shows bright and dark areas in the focused images obtained by the aperture displacement corresponding to the above illustration in (a). The aperture-beam relationships are indicated by the symbols.



(a)

(c)

(b)

Figure 20. Contrast in the focused image obtained by the Foucault method. The arrows in (a), (b) and (c) show the directions of the objective aperture displacement.

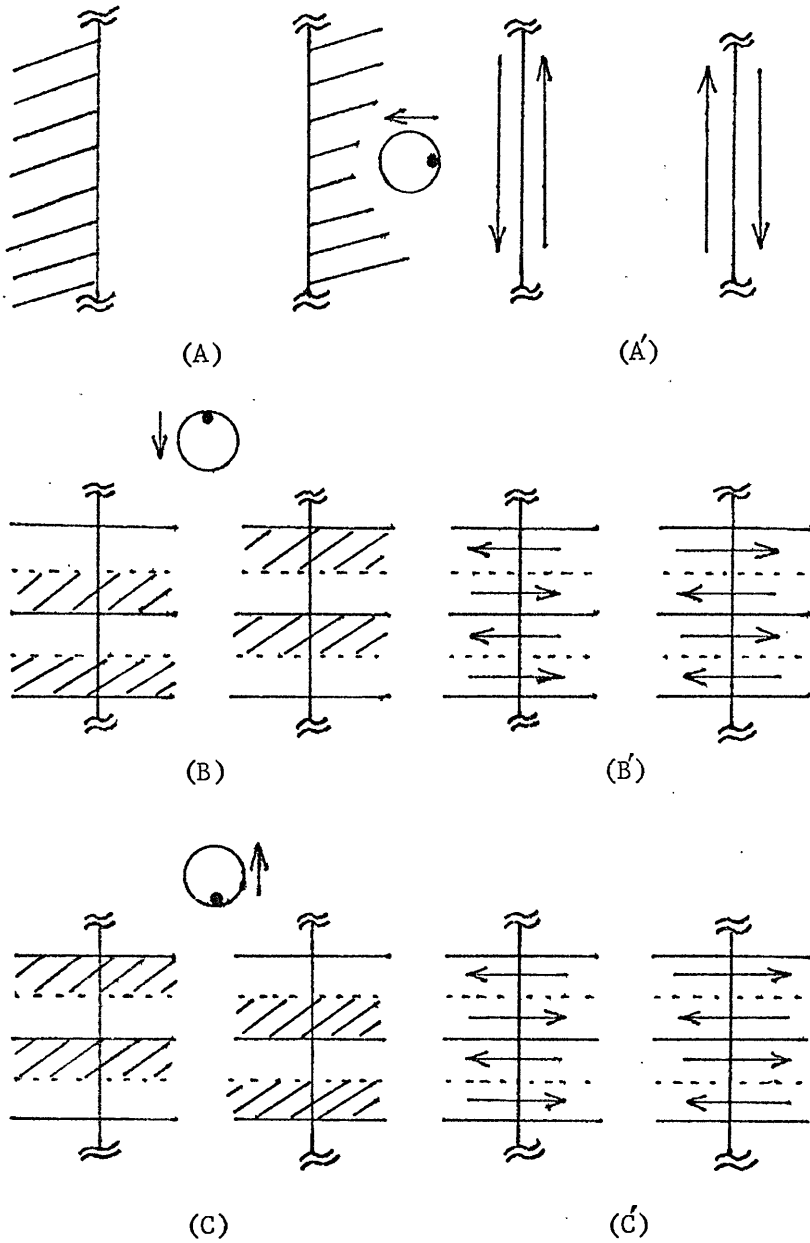
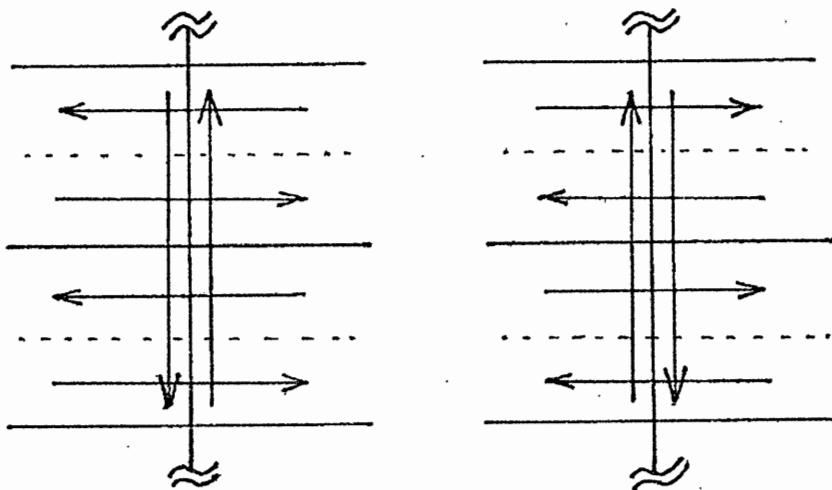
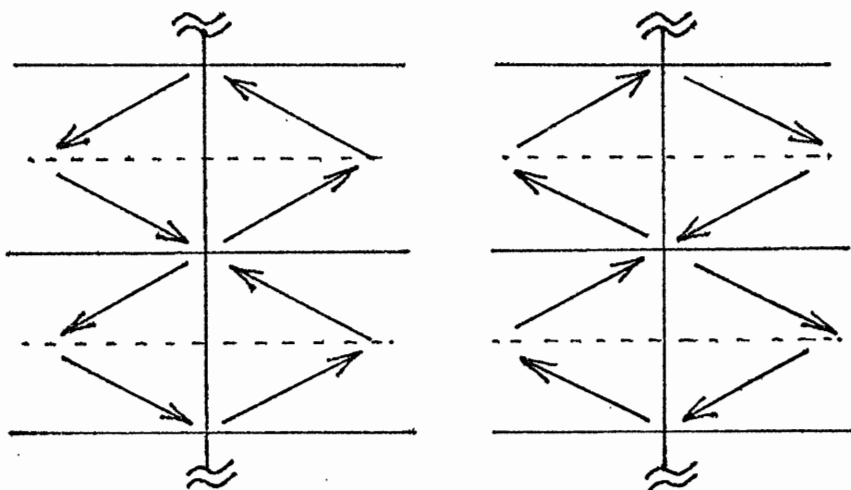


Figure 21. (A), (B) and (C) Show illustrations of the contrast in Figure 20(a), (b) and (c). (A'), (B') and (C') Indicate the directions of local magnetizations which account for the corresponding contrast in (A), (B) and (C), respectively.



(a)



(b)

Figure 22. (a) Shows the combination of local magnetization obtained in Figure 21. (b) Indicates the vectorial sum of local magnetization in (a).

4. A Study of the Effect on Crosstie Walls of an In-plane Magnetic Field (30).

Studies of the crosstie walls in applied magnetic fields have been made by a number of investigators (e.g. 14, 15, 16, 17, 18) using the Bitter technique. We have studied the effect of applying an in-plane field to crosstie walls by the ETEM Lorentz method (30). The specimen, a thin iron film, was subjected to an in-plane magnetic field prior to insertion in an ETEM. The field strength was increased by increments and the specimen observed after each increase.

In this experiment the in-plane magnetic fields were applied at right angles to crosstie main walls. The crosstie density for a $\sim 250 \text{ \AA}$ iron film began to decrease gradually as the applied magnetic field was increased, and the slope of the density curve, as shown in Figure 23, was fairly large in the 15 Oe range. The crossties had been obliterated by 38 Oe. A sequence of observations between 0 and 40 Oe was made in Figure 24. Where crossties disappeared in the in-plane application, the main wall was disturbed and began to move, and a twisted type of domain emerged. The same effect appeared in a slightly thinner specimen ($\sim 200 \text{ \AA}$) at 18 Oe as shown in Figure 25. Thus, it seems that the critical field strength necessary to disrupt the main wall depends strongly on specimen thickness.

Another interesting observation was made in this study, in which the crosstie main wall-wall distance dropped suddenly just before the crossties were obliterated (Figures 23 and 24).

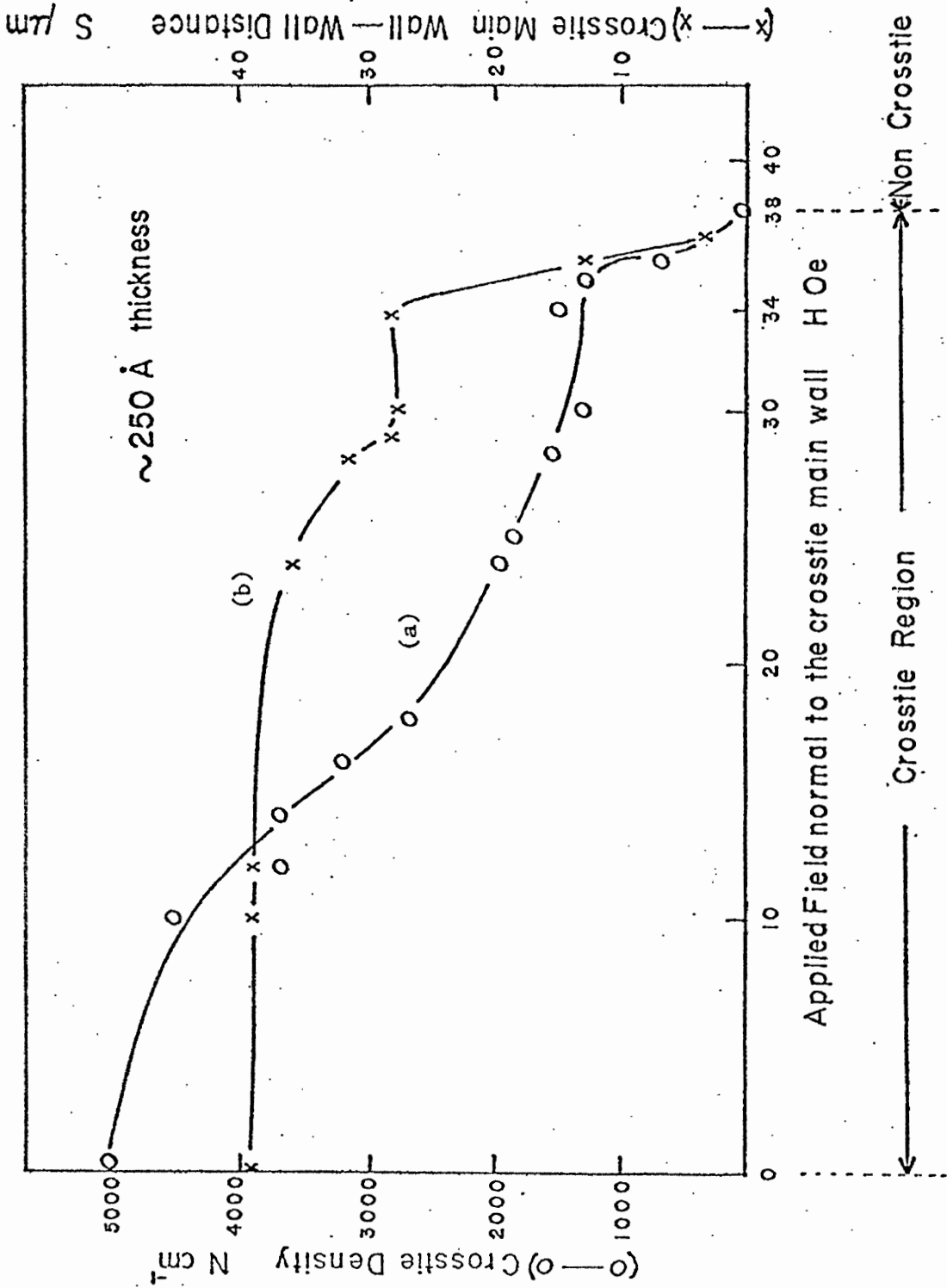
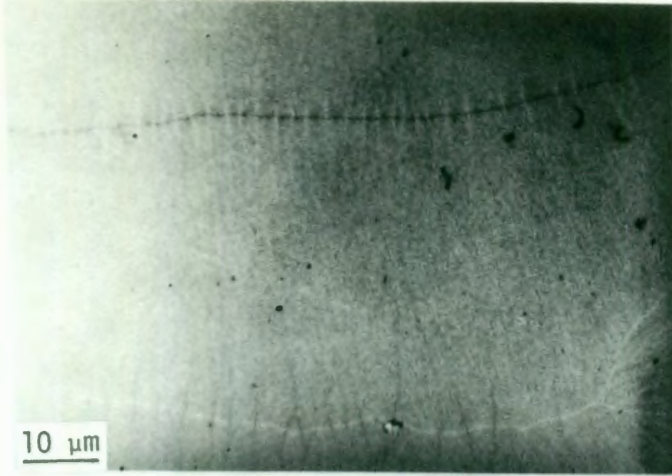


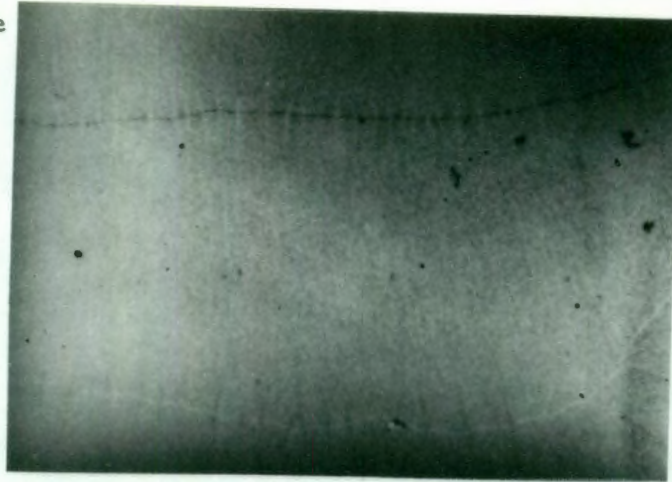
Figure 23. Relation between (a) crosstie density and applied field normal to the crosstie main wall, and (b) field dependence on crosstie main wall-wall distance.

0 Oe
↓



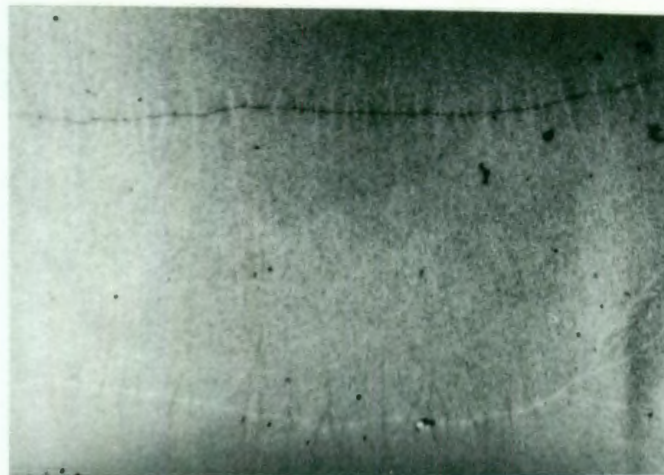
(a)

12 Oe
↓



(b)

18 Oe
↓



(c)

Figure 24(a), (b), (c). Field dependence of crosstie walls in an iron thin film by the underfocus method. The directions of in-plane field strength in (a), (b) and (c) are indicated by arrows. (Film thickness $\sim 250 \text{ \AA}$)

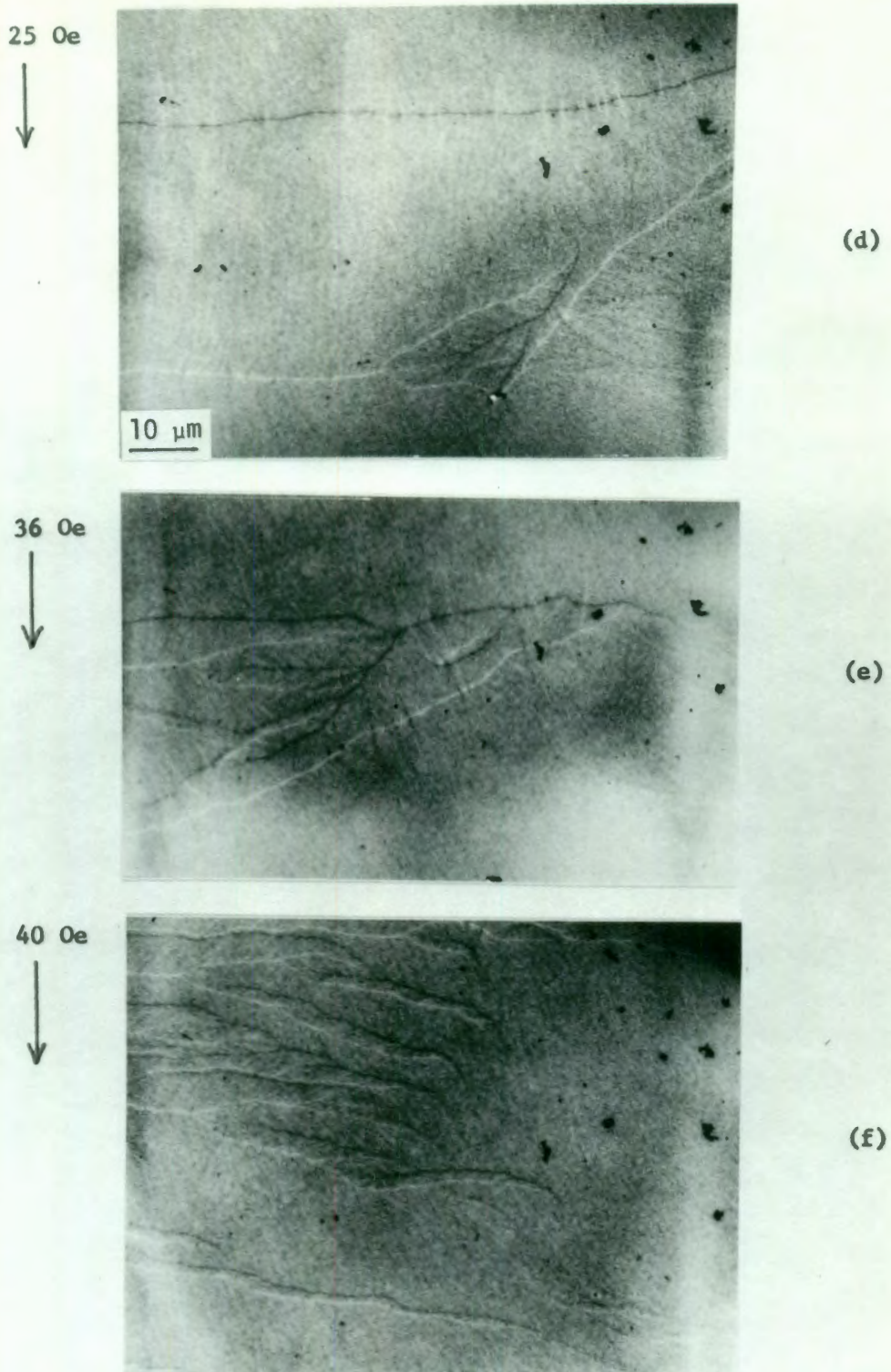


Figure 24(d), (e), (f). Field dependence of crosstie walls in an iron thin film by the underfocus method. The directions of in-plane field strength in (d), (e) and (f) are indicated by arrows. (Film thickness $\sim 250 \text{ \AA}$)

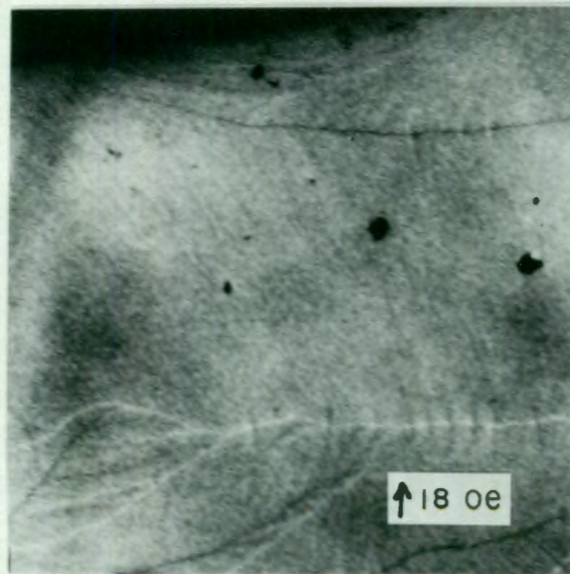
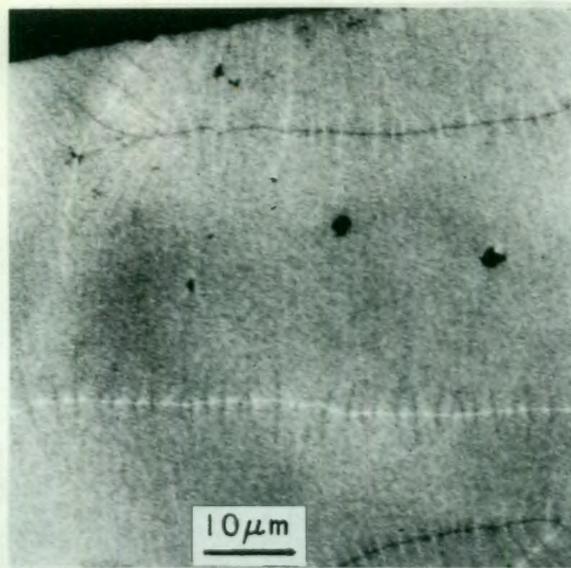


Figure 25. Field dependence of crosstie walls in an iron thin film by the underfocus method. Film thickness was $\sim 200 \text{ \AA}$.

5. A study of Bloch line-crosstie Annihilation in Applied Magnetic Field

The purpose of this study is to observe how Bloch lines and crossties behave in the in-plane field application. In-plane fields were applied at right angles to crosstie main walls in a $\sim 200 \text{ \AA}$ iron thin film.

The micrographs shown in Figure 26(a), (b), and (c) were taken by the ETEM underfocus method. The information in Figure 26 is shown schematically in Figure 27. Figure 27(a) exhibits Bloch line-crosstie pairs with no applied field. The in-plane field 2 Oe is the threshold field which causes the Bloch line-crosstie annihilation as shown in Figure 27 (b). A Bloch line on the right between a crosstie 'a' and 'b' in Figure 27 (b) is pushed to the left by the in-plane field in the direction of the arrow. The completion of a Bloch line-crosstie annihilation can be observed at 4 Oe as illustrated in Figure 27(c).

A Bloch line-crosstie pair annihilation process can also be seen at higher fields. This process is repeated until the crosstie density has been reduced to the point where main wall motion occurs.

It is also observed that Bloch line-shorter crosstie pairs annihilate faster than Bloch line-longer crosstie pairs.

The micrographs of several Bloch line-crosstie pairs in Figure 26 observed by the underfocus method show evidence indicating a clockwise rotation of magnetization about each Bloch line.

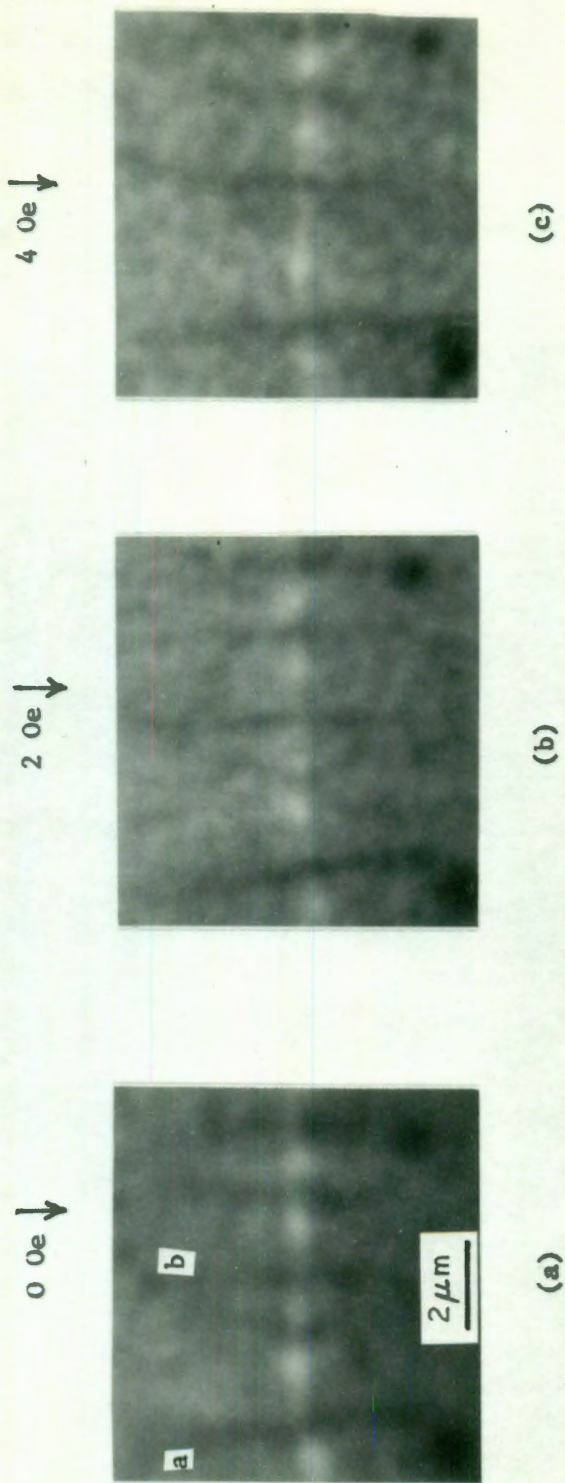


Figure 26. Electron micrographs of a Bloch line-cross-tie annihilation in the in-plane field dependence. (Iron thin film, $\sim 200 \text{ \AA}$ of thickness) The underfocus method was used.

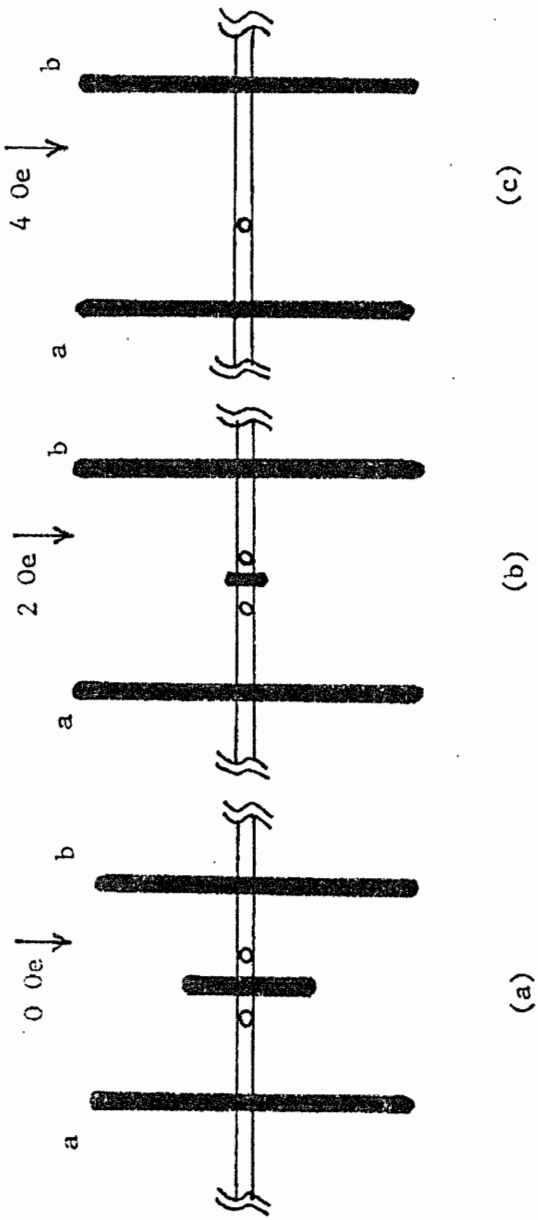


Figure 27. Illustration of a Bloch line-cross-tie annihilation in the in-plane field dependence in Figure 26. (Iron thin film, $\sim 200 \text{ \AA}$ of thickness) The underfocus method was used.

6. A Study of Twisted Type Domains and Crosstie-twisted Boundaries

S. Middelhoek (31) reported that structures such as Néel wall, crosstie wall and Bloch wall are all dependent upon thickness, and that the most stable domain structure for permalloy films between 0 and $\sim 900 \text{ \AA}$ thick was the crosstie wall structure. The crosstie wall-Bloch wall transition occurs with the thickness ($\sim 900 \text{ \AA}$) as shown in Figure 28. According to Middelhoek's theory concerning permalloy thin film, it may be possible to determine a similar structural dependence on thickness in case of iron thin films.

We first observed 180° domain walls and crosstie walls in films $\sim 200 \text{ \AA}$ thick. Subsequently we observed twisted domains as well as crosstie-twisted boundaries in $\sim 200 \text{ \AA}$ films as shown in Figure 29 and 30. In this study we found that twisted domains made their appearance where crossties were obliterated during field application (shown in Section 4). The twisted domains in Figure 29 and 30, however, occurred in specimens to which a magnetic field had not been deliberately applied, which may have been exposed inadvertently to a field. The interesting characteristic of these boundaries is that crosstie regions appear along the twisted boundaries alternately in a periodic manner. Additional micrographs (Figure 31) of the same crosstie-twisted boundaries as in Figure 30 were taken by the Foucault method.

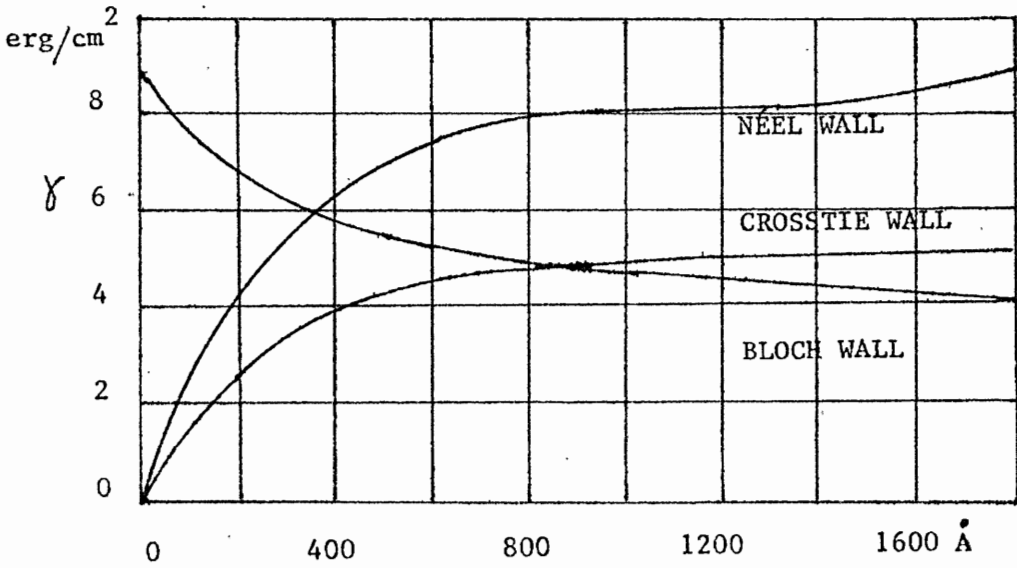


Figure 28. Energy per unit area of a Bloch wall, a Néel wall and a crosstie wall as a function of the film thickness (31). (Permalloy thin films)

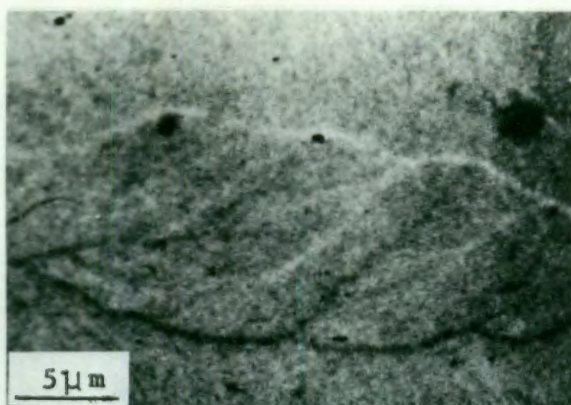


Figure 29. Twisted domains which occur at $\sim 200 \text{ \AA}$ of thickness in iron thin film. Taken by the underfocus method.

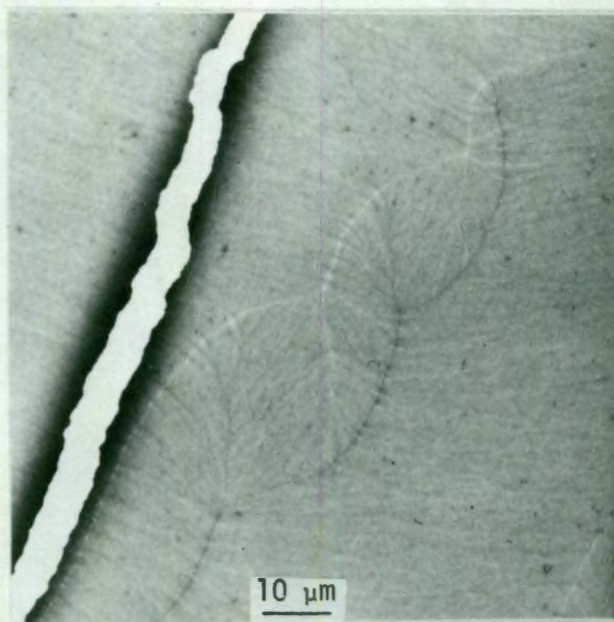


Figure 30. Crosstie-twisted boundaries which occur at $\sim 200 \text{ \AA}$ of thickness in iron thin film. Taken by the underfocus method.

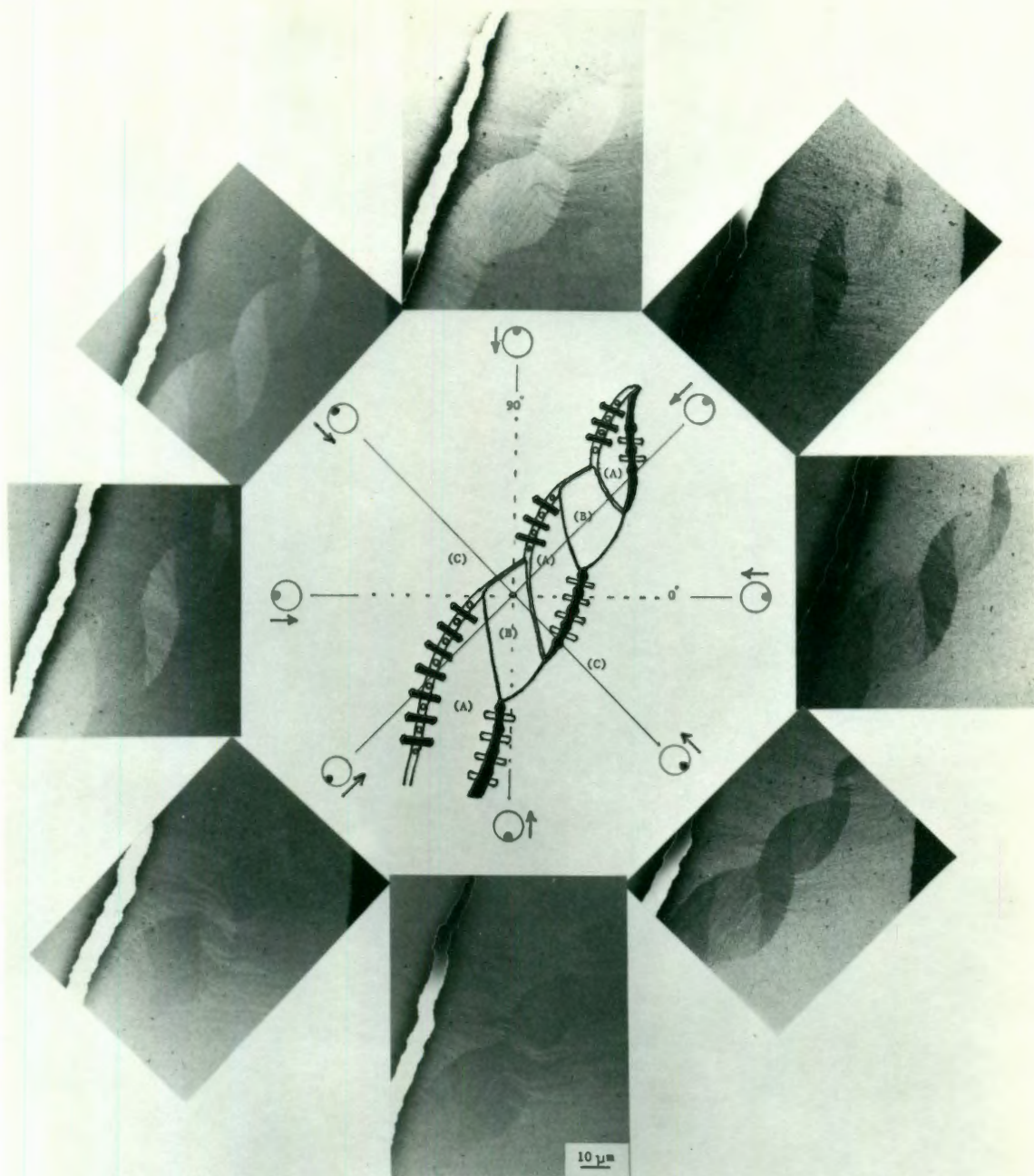


FIGURE 31. THE SAME CROSSTIE-TWISTED BOUNDARIES IN FIGURE 30 WERE SUBSEQUENTLY TAKEN BY THE FOUCAULT METHOD, AND THE OBJECTIVE APERTURE STOP WAS INSERTED AT EVERY 45° AZIMUTHAL ROTATION OF THE SPECIMEN.

The diagram in Figure 32 is an illustration of crosstie-twisted boundaries observed by the underfocus method in Figure 30. One of the interesting characteristics of this observation is to visualize easily, thick, bright and dark boundaries as well as thin, bright and dark boundaries. There are thick boundaries between regions (A) and (C), and thin boundaries between regions (B) and (C), and regions (A) and (B) in Figure 32. Thick boundaries indicate to us that vectorial directions of magnetization are parallel to the domain wall as shown in Figure 33(a) and (b). Thin boundaries represent that vector components parallel to the domain wall are less than in cases (a) and (b) as illustrated in Figure 33(c) and (d). We can obtain a possible configuration of magnetizations in crosstie-twisted boundaries with these conditions. To draw a final conclusion, however, some of the photographs observed by the Foucault method in Figure 31 are taken into account. By insertion of an aperture in the direction indicated by the arrow at the 0° position, regions (A) become dark, (B) intermediate dark and (C) bright as shown in Figure 31. Considering thick, bright and dark boundaries between regions (A) and (C) observed by the underfocus method, a possible structure of the domain wall in regions between (A) and (C) are 180° domain walls as shown in Figure 33(a) and (b). Intermediate dark areas of (B) indicate to us that in each region (B) a component of magnetization normal to the direction of aperture displacement to make these regions appear darker than regions (C) when the aperture is inserted at the 0° position. By insertion of an aperture in the direction indicated by the arrow at the 90° position as shown in Figure 31, regions (A) and (B) become bright, and region (C) dark. This fact tells us that there exist

no vectorial components of magnetization to make regions (A) and (B) dark. But there is a vectorial component of magnetization normal to the direction of aperture displacement which makes the region (C) dark with insertion of the aperture at the 90° position. Taking into account all these conditions, a possible configuration of magnetization in crosstie-twisted boundaries was determined and is shown in Figure 34.

Our findings in this study are : 1. Crosstie-twisted boundaries are combinations of 180° domain walls and 90° domain walls; 2. Crossties do not emerge along 90° domain walls, but along 180° domain walls; 3. Crosstie density along 180° domain walls is approximately 4500 cm^{-1} .

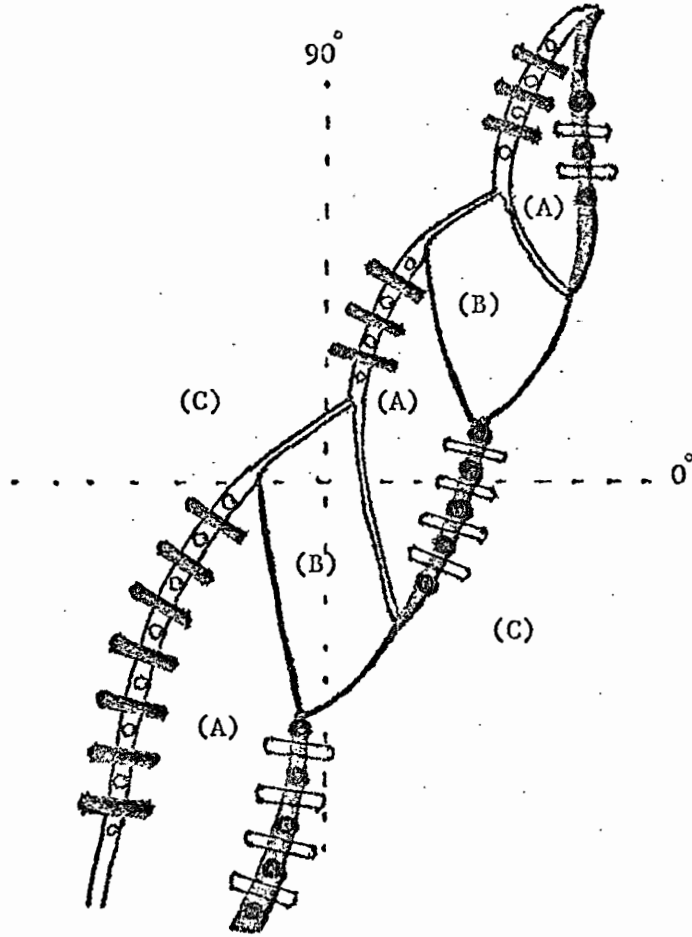


Figure 32. Illustration of crosstie-twisted boundaries observed by the underfocus method in Figure 30.

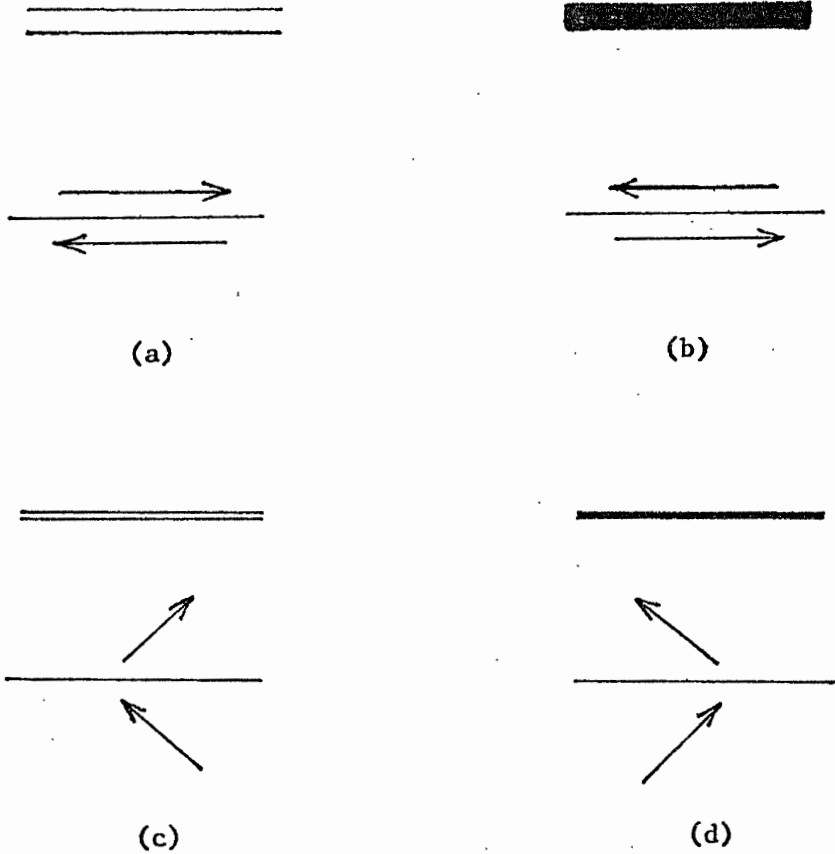


Figure 33. Relation between the contrast of a thick bright line and directions of local magnetization (a), and between the contrast of a thick dark line and directions of local magnetization (b). Thin bright and dark lines in (c) and (d) indicate to us that vectorial components of magnetization parallel to the boundaries are less than in (a) and (b).
 (Electrons into paper and underfocus method)

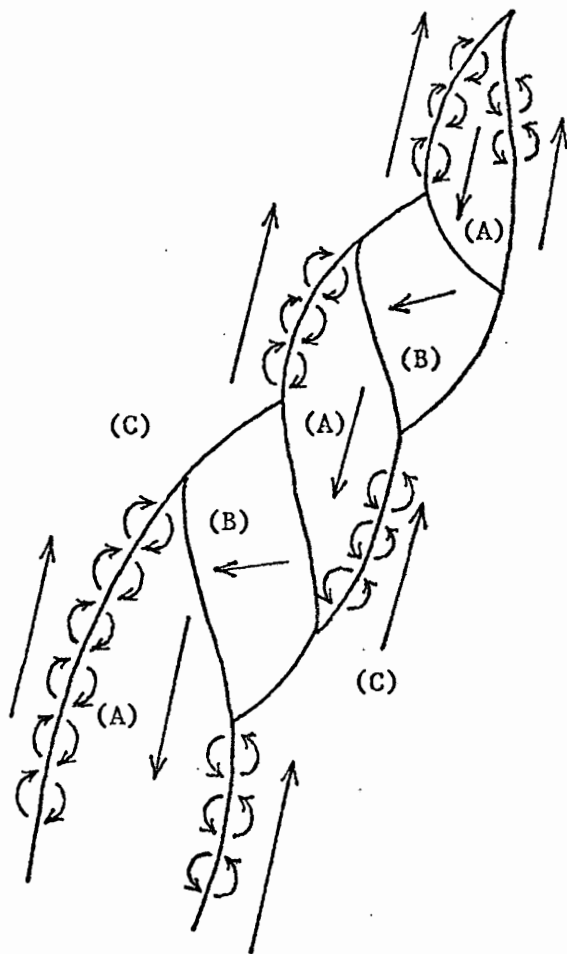


Figure 34. Possible configuration of magnetization of crosstie-twisted boundaries. Crosstie-twisted boundaries are combinations of 180° domain walls and 90° domain walls. Crossties do not emerge along 90° domain walls, but along 180° domain walls. Crosstie density along 180° domain walls is approximately 4500 cm^{-1} .

CHAPTER IV

SUMMARY AND CONCLUSIONS

Electron microscopy with ETEM is a promising method to observe magnetic domains at high resolution without disturbance from stray magnetic fields.

Using the Lorentz and Foucault methods to give complementary information, it is possible to determine directions of local magnetization.

When in-plane magnetic fields are applied normal to crosstie main walls, the crosstie density is reduced. This process involves annihilation of Bloch line-crosstie pairs. Where the crossties have disappeared, a twisted type of domain forms.

We also observed crosstie-twisted boundaries. It is found that crosstie-twisted boundaries consist of combinations of 90° domain walls, 180° domain walls and crosstie walls. Crossties are found along the 180° domain walls but not along the 90° domain walls. The crosstie density along 180° domain walls is approximately 4500 cm^{-1} .

References

1. Bitter, F. Phys. Rev. 38, 1903, 1931.
2. Bitter, F. Phys. Rev. 41, 507, 1932.
3. Williams, H. J., Bozorth, R. M. and Shockley, W. Phys. Rev. 75, 155, 1948.
4. Hale, M. E., Fuller, H. W. and Rubinstein, H. J. Appl. Phys. vol.30. 5, 789, 1959.
5. Fuller, H. W., and Hale, M. E. J. Appl. Phys. vol.31. 10, 1699, 1960.
6. Fuller, H. W., and Hale, M. E. J. appl. Phys. vol.31. 2, 238, 1960.
7. Silcox, J. Phil. Mag. 8, 7, 1963.
8. Petrov, V. I., Spivak, G. V., and Pavlyuchenko, O. P. Soviet Physics Uspekhi. vol.15. 1, 66, 1972.
9. Torok, E. J. AIP Conf. Proc. M.M.M. 24, 753, 1974.
10. Blackburn, M. J. S., and Ferrier, R. P. J. Appl. Phys. vol.39. 2, 1163, 1968.
11. Cohen, M. S. J. Appl. Phys. vol.34. 4, 1221, 1963.
12. Leamy, H. J., Wakiyama, T., and Chin, G. Y. AIP Conf. Proc. M.M.M. 24, 755, 1974.
13. Mahajan, S., and Olsen, K. M. AIP Conf Proc. M.M.M. 24, 743, 1974.
14. Huber, E. E. Jr., Smith, D. O., and Goodenough, J. B. J. Appl. Phys. vol.29. 3, 294, 1958.
15. Moon, R. M. J. Appl. Phys. vol.30. 4, 82S, 1959.
16. Gomi, Y., and Odani, Y. J. Phys. Soc. Japan. 15, 535, 1960.
17. Rubiustein, H., and Spain, R. J. J. Appl. Phys. vol.31. 5, 306S, 1960.

18. Methfessel, S., Middelhoek, S., and Thomas, H.
IBM. J. Res. Dev. vol.4. 2, 96, 1960.
19. Schwee, L. J. AIP Conf. Proc. Part 2. 10, 996, 1972.
20. Schwee, L. J., Irons, H. R., and Anderson, W. E.
AIP Conf. Proc. M.M.M. 1383, 1973.
21. Cosimini, G. J., Johnson, L. H., Lo, O. S., Nelson, G. F.,
Paul, M. C., and Torok, E. J. J. Appl. Phys.
vol.49. 3, 1828, 1978.
22. Lo, D. S., Olson, A. L., Olson, C. D., Oredson, H. N.
Simon, W. J., and Torok, E. J. J. Appl. Phys.
vol.38. 3, 1344, 1967.
23. Torok, E. J., Olson, C. D., Oredson, H. N., and Simon, W. J.
J. Appl. Phys. vol.40. 3, 1222, 1969.
24. Paul, D. I., Marti, J., and Valadez, L. AIP Conf. Proc.
M.M.M. 1377, 1973.
25. Cohen, M. S. J. Appl. Phys. vol.39. 2, 1149, 1968.
26. Puchalska, I. B. J. Appl. Phys. vol.50. 3, 2242, 1979.
27. Schwee, L. J., Anderson, W. R., Liu, Y. J., and Lee, R. N.
J. Appl. Phys. vol.49. 3, 1831, 1978.
28. Lee, R. N., Anderson, W. E., Liu, Y. J. and Schwee, L. J.
IEEE Trans. Mag. vol.MAG-14. 5, 1076, 1978.
29. Lo, D. S., Benrud, V. M., Cosimini, G. J., Johnson, L. H.,
Nelson, G. F., Paul, M. C., and Torok, E. J.
J. Appl. Phys. vol.50. 3, 2295, 1979.
30. Karamon, H. 37th Ann. Proc. Electron Microscopy Soc. America.
670, 1979.
31. Middelhoek, S. J. Appl. Phys. vol.34. 4, 1054, 1963.